

Review

Nonlinearity in piezoelectric ceramics

D. A. HALL

Materials Science Centre, University of Manchester and UMIST, Manchester M1 7HS, UK
E-mail: mblssdah@fs2.mt.umist.ac.uk

The paper presents an overview of experimental evidence and present understanding of nonlinear dielectric, elastic and piezoelectric relationships in piezoelectric ceramics. This topic has gained an increasing recognition in recent years due to the use of such materials under extreme operating conditions, for example in electromechanical actuators and high power acoustic transducers. Linear behaviour is generally confined to relatively low levels of applied electric field and stress, under which the dielectric, elastic and piezoelectric relationships are described well by the standard piezoelectric constitutive equations. Nonlinear relationships are observed above certain 'threshold' values of electric field strength and mechanical stress, giving rise to field and stress-dependent dielectric (ϵ), elastic (s) and piezoelectric (d) coefficients. Eventually, strong hysteresis and saturation become evident above the coercive field/stress due to ferroelectric/ferroelastic domain switching. The thermodynamic method provides one approach to describing nonlinear behaviour in the 'intermediate' field region, prior to large scale domain switching, by extending the piezoelectric constitutive equations to include nonlinear terms. However, this method seems to fail in its prediction of the amplitude and phase of high frequency harmonic components in the field-induced polarisation and strain waveforms, which arise directly from the nonlinear dielectric and piezoelectric relationships. A better fit to experimental data is given by the empirical Rayleigh relations, which were first developed to describe nonlinear behaviour in soft magnetic materials. This approach also provides an indication of the origins of nonlinearity in piezoelectric ceramics, in terms of ferroelectric domain wall translation (at intermediate field/stress levels) and domain switching (at high field/stress levels). The analogy with magnetic behaviour is also reflected in the use of Preisach-type models, which have been successfully employed to describe the hysteretic path-dependent strain-field relationships in piezoelectric actuators. The relative merits and limitations of the different modelling methods are compared and possible areas of application are identified. © 2001 Kluwer Academic Publishers

1. Background and aims

Polycrystalline piezoelectric ceramics are by necessity also ferroelectric, since it is necessary to be able to induce a preferred direction of polarisation within a piezoceramic component in order to obtain a macroscopic piezoelectric response. By definition, any ferroelectric material will exhibit a nonlinear P - E (polarisation-electric field) relationship at sufficiently high field strengths, which is associated with the reorientation of the spontaneous polarisation by the electric field. Therefore, it follows that the dielectric properties of piezoelectric ceramics are inherently nonlinear. Reorientation of the spontaneous polarisation also produces an associated change in strain, giving rise to a nonlinear piezoelectric x - E (strain-electric field) response. The reorientation of 90° ferroelectric domains (for tetragonal ferroelectrics) or $71/109^\circ$ ferroelectric domains (for rhombohedral ferroelectrics) under an applied mechanical stress means that the x - X (strain-

stress) relationships of piezoelectric ceramics are also inherently nonlinear.

The effective dielectric, elastic and piezoelectric coefficients of piezoelectric ceramics show pronounced dependencies on the applied electric field strength and stress intensity, due to variations in the ferroelectric domain wall contributions to those properties. It is somewhat surprising then to note that the majority of the published data on commercial piezoelectric ceramics assumes a perfectly linear response according to the piezoelectric constitutive equations:

$$x_m = S_{mn}^E X_n + d_{im}^X E_i \rightarrow x_m = S_{mn}^E X_n + d_{im}^X E_i \quad (1)$$

$$D_i = d_{im}^E X_m + \epsilon_{ij}^X E_j \quad (2)$$

Here, D is the dielectric displacement, ϵ the dielectric permittivity, s the compliance and d the piezoelectric charge/strain coefficient. Superscripts indicate the independent variable held constant while subscripts

indicate components of the vector or tensor quantities. Summation over all possible components of X or E is assumed for repeated subscripts.

The linear description provides a reasonable approximation of the functional characteristics of piezoelectric ceramics at low levels of applied electric field and stress, but becomes increasingly inaccurate as the field and stress levels increase. The discrepancies between published data (usually measured at low field levels) and the functional behaviour of piezoelectric ceramics under 'real world' operating conditions is immediately apparent in piezoelectric actuators, where relatively high electric field levels ($\sim 0.5 \text{ kV mm}^{-1}$) are necessary to obtain a useful actuation effect. Under such conditions, the effective piezoelectric strain coefficient of a *soft* PZT ceramic can easily rise to a level that is 100% greater than the nominal value, as shown in Fig. 1 below. Pronounced nonlinearity and hysteresis in the strain-field relationship are also evident under such conditions.

Reductions in the thickness of piezoceramic layers, for example in cofired multilayer actuators and thick/thin film piezoelectric devices, has enabled larger strains to be developed at moderate voltage levels. However, this has also meant that the nonlinear characteristics are all the more pronounced. Therefore, the

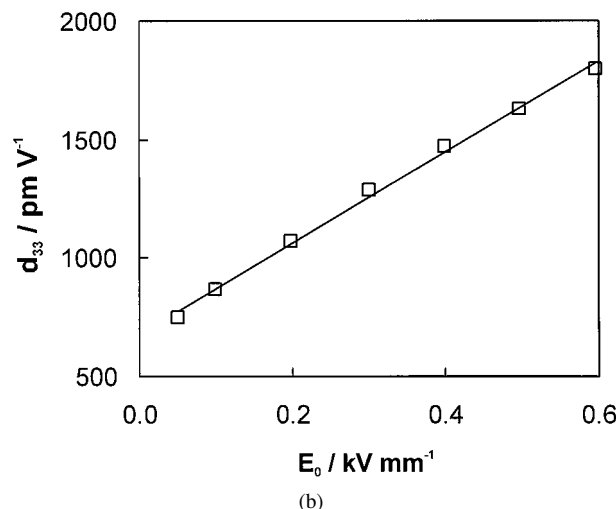
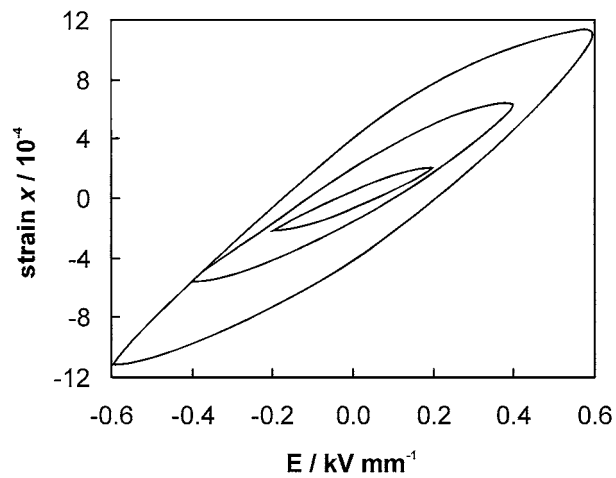


Figure 1 (a) Strain-electric field relationship and (b) increase in effective d_{33} coefficient with field amplitude for soft PZT ceramic (data provided by M Stewart, NPL).

practical significance of the nonlinear behaviour of piezoelectric ceramics, and the need to develop improved models for their functional characteristics, have gained an increasing recognition. As a result of this, many studies of nonlinearity in ferroelectrics have been carried out during the past 10 years. Most of these have been concerned with nonlinearity in the dielectric properties, since these are the most straightforward to determine by purely electrical measurements.

Some investigations have been carried out to establish the extent of nonlinearity in the direct and converse piezoelectric properties of ferroelectric ceramics. In most cases, these studies considered the influence of electric field amplitude (for the converse effect) or mechanical stress level (for the direct effect) in isolation. Considering the combined effects of electrical and mechanical loading, as will be necessary for piezoelectric actuators acting against an external mechanical load, leads to further complexity, as is discussed in Section 3 below.

The aim of this review is to provide a state of the art overview of the characteristic features of nonlinearity in piezoelectric ceramics, together with an insight into the underlying mechanisms responsible for nonlinear behaviour. Suitable approaches for modelling the nonlinear dielectric, piezoelectric and elastic (mechanical) properties are also considered in the final sections of the review.

2. Experimental studies of nonlinearity in piezoelectric ceramics

2.1. Extrinsic contributions to low field dielectric, piezoelectric and elastic properties

It was recognised in the earliest studies on ferroelectrics that the movement of ferroelectric domain walls should make a significant contribution to the dielectric properties [1]. This was most evident in the saturated ferroelectric P - E hysteresis loop where the reversal, or 'switching', of domains under the influence of an applied electric field gave rise to a significant remanent polarisation and a pronounced hysteresis loss. At lower field levels, the reversible vibration of domain walls about an equilibrium position was also supposed to provide a significant contribution to the dielectric properties. Lewis referred to the domain switching and domain wall vibration mechanisms as *macrohysteresis* and *microhysteresis* respectively [2]. It is usual practise to distinguish between such *extrinsic* ferroelectric domain-related polarisation mechanisms and the *intrinsic* ionic (or volume) response that would be obtained in a single domain, single crystal ferroelectric.

Both the intrinsic and extrinsic mechanisms contribute to the real 'in-phase' components of field-induced strain and dielectric displacement, whereas the imaginary lossy components are due solely to the extrinsic mechanisms. Thus, we can represent the dielectric, piezoelectric and elastic coefficients as [3]:

$$\begin{aligned} \varepsilon^* &= \varepsilon' - j\varepsilon'' & \varepsilon' &= \varepsilon'_{in} + \varepsilon'_{ex} & \varepsilon'' &= \varepsilon''_{ex} \\ d^* &= d' - jd'' & d' &= d'_{in} + d'_{ex} & d'' &= d''_{ex} \\ s^* &= s' - js'' & s' &= s'_{in} + s'_{ex} & s'' &= s''_{ex} \end{aligned} \quad (3)$$

where ‘*’ denotes a complex quantity and the indices ‘in’, ‘ex’ refer to intrinsic and extrinsic contributions respectively.

It should be noted that the extrinsic ferroelectric domain-related contributions to the dielectric, piezoelectric and elastic properties can be further subdivided into those due to domain wall vibration, domain wall translation, and domain switching. It is usually assumed that only domain wall vibration will provide a contribution for field levels below approximately 10 V mm^{-1} . The methods used by various researchers to quantify the linear domain wall vibration contributions at low field levels are summarised below, while subsequent sections are concerned with the nonlinear effects associated with domain wall translation and domain switching.

In general, the intrinsic and extrinsic contributions to any given property can be separated by considering their variations as a function of some externally-controlled variable. Most of the investigations on ferroelectric ceramics have studied the effects of either frequency of the measuring field, temperature, or ageing time. Each of these methods is described in further detail below.

The frequency-dependence of dielectric properties in ferroelectric ceramics usually reveals the presence of a relaxation step at a frequency $f_0 \sim 10^9 \text{ Hz}$, which is thought to be associated with the domain wall vibration contribution. Von Hippel described some of the early studies of this effect in ferroelectrics [1]. Later work by Poplavko *et al.* demonstrated that in barium titanate ceramics a relaxation step of around 600 in the dielectric permittivity could be observed at a frequency of approximately 4 GHz, as shown in Fig. 2 [4].

If this data is ascribed to the loss of the domain wall contribution at high frequencies, then the remaining permittivity value at frequencies higher than f_0 can be identified as being due solely to the intrinsic ionic response, which is assumed to be independent of frequency. This enables an estimation of the intrinsic and extrinsic contributions at frequencies below f_0 as approximately 500 and 600 respectively.

Similar studies have been carried out subsequently on other BaTiO_3 and PZT-based ceramics [5–8]. Although similar relaxations steps were observed, their origin has been questioned and some alternative mechanisms suggested [5, 8]. For the present purpose, the exact origin

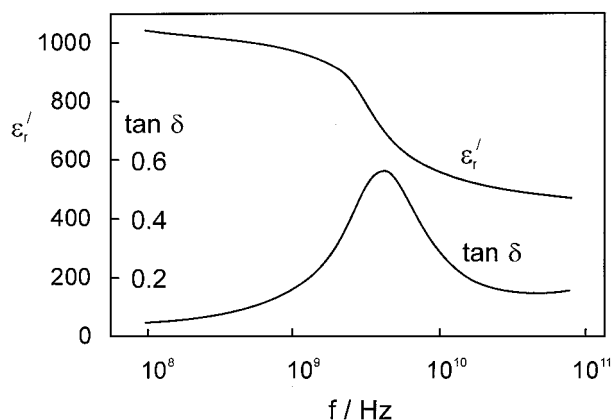


Figure 2 Frequency dependence of dielectric properties of barium titanate ceramics, after Poplavko *et al.* [4].

of the relaxation step is not of great importance since this method is only appropriate for measurement of the dielectric properties and the measurement techniques themselves present significant practical problems.

The variation of the dielectric, piezoelectric and elastic properties of ferroelectrics as a function of temperature has been studied by several authors as a means of separating the intrinsic and extrinsic contributions. The basic principle of this method is that the domain wall contributions are frozen out at temperatures close to absolute zero. Thus, the intrinsic contribution can be determined exactly at absolute zero. If an approximate form of the temperature-dependence of the intrinsic contribution can be derived, then this enables a determination of the extrinsic contribution at any given temperature.

Typical results obtained by Herbiet *et al.* using this method are shown in Fig. 3 [3]. In this case, the dielectric, piezoelectric and elastic coefficients ϵ_{33} , d_{31} and s_{11} were measured simultaneously by using a length-extensional piezoelectric resonator with a resonant frequency of approximately 150 kHz [9].

A similar method was utilised by Zhang *et al.* to determine the intrinsic and extrinsic contributions to the ϵ_{33} , d_{33} and d_{31} coefficients of soft PZT ceramics [10]. Their analysis was based on the simple hypothesis that the extrinsic contribution to the hydrostatic piezoelectric coefficient d_h should be zero, since the motion of domain walls does not involve a change in volume. This enabled a separation of the intrinsic and extrinsic contributions to d_{33} and d_{31} , as shown in Fig. 4.

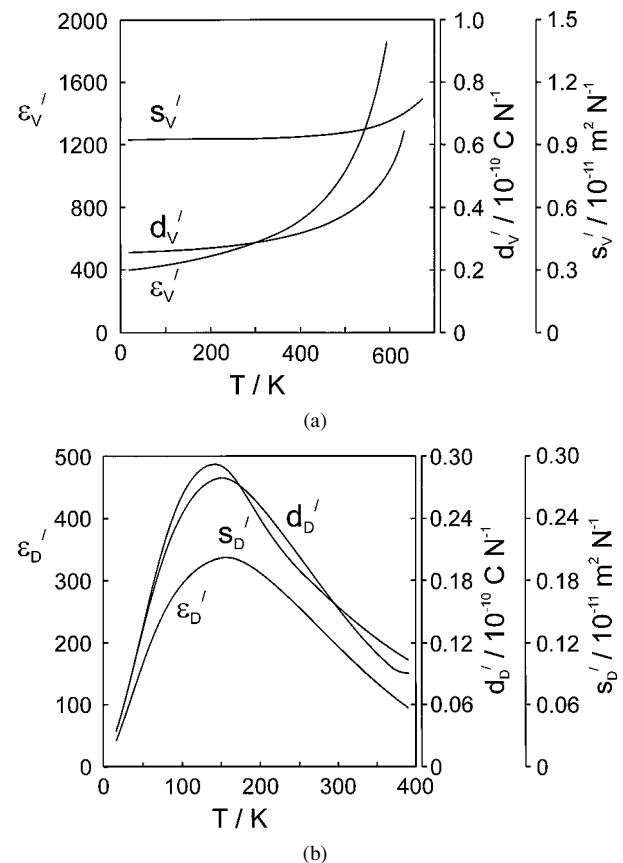


Figure 3 Determination of (a) intrinsic and (b) extrinsic contributions to ϵ_{33} , d_{31} and s_{11} of an undoped PZT ceramic as a function of temperature, after Herbiet *et al.* [3].

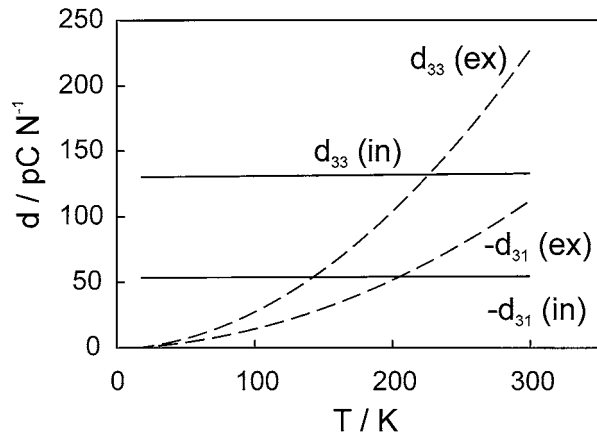


Figure 4 Separation of intrinsic and extrinsic contributions to d_{33} and $-d_{31}$ coefficients of soft PZT ceramics, after Zhang *et al.* [10].

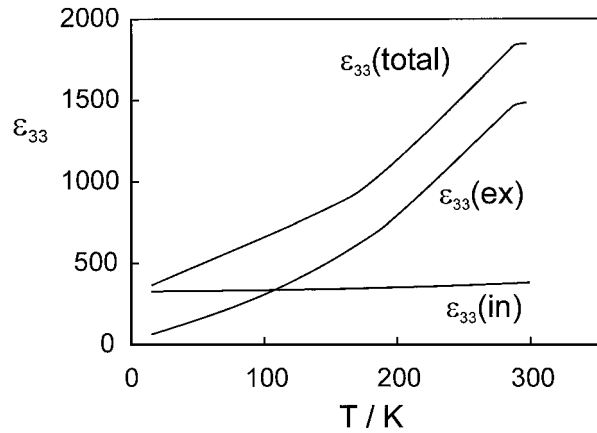


Figure 5 Temperature dependence of the intrinsic and extrinsic contributions to the dielectric permittivity for soft PZT ceramics, after Zhang *et al.* [10].

Furthermore, by utilising the relationships between ϵ_{33} , d_{33} , d_{31} and d_h , via the electrostrictive coefficients Q_{11} , Q_{12} and Q_h , it was possible to estimate the intrinsic and extrinsic contributions to ϵ_{33} , as shown in Fig. 5. It is clear from the published results that the extrinsic contributions to ϵ , d , and s of soft PZT ceramics at room temperature and low field levels are significant and may account for 50–80% of the overall response. There are clearly differences in the temperature dependence of the extrinsic components of ϵ and d , as reported by these authors. The origin of this discrepancy is unclear at present, but may be related to differences in the measurement method or in the different materials under investigation in each case.

The domain wall contributions to the properties of *hard* piezoceramics are likely to be much smaller than those in soft piezoceramics. In fact, the dopants (acceptors or donors) that are used to modify the properties of PZT ceramics are thought to act largely by modifying the extrinsic response [10]. Donor dopants (e.g. La, Nb) are found to facilitate ferroelectric domain wall motion and result in soft PZT ceramics with high piezoelectric coefficients and relatively high dielectric loss [11]. In contrast, acceptor dopants (e.g. Mn, Fe) inhibit ferroelectric domain wall motion and result in hard PZT ceramics with lower piezoelectric coefficients

and much reduced dielectric loss. These effects are attributed largely to the presence of oxygen vacancies, the concentration of which is increased by acceptors and suppressed by donors.

Paired acceptor ion-oxygen vacancy defect associates e.g. $Ni_{Ti}'' - V_O^{\bullet\bullet}$ constitute dipolar defects that retain a limited mobility at ambient temperatures. These defects can be reoriented under the influence of the local domain polarisation, causing a gradual stabilisation of the ferroelectric domain structure and a reduction of domain wall mobility. This gives rise to ageing effects in ferroelectrics, characterised by gradual reductions in the dielectric, piezoelectric and elastic coefficients after a high temperature electroding or poling operation [3, 12].

These processes provide another means of determining the extrinsic contributions, since the intrinsic response is assumed to be independent of ageing time. Thus, the time-dependent dielectric, piezoelectric and elastic coefficients can be written as:

$$\begin{aligned} \epsilon'(t) &= \epsilon'_{in} + \epsilon'_{ex}(t) & \epsilon''(t) &= \epsilon''_{ex}(t) \\ d'(t) &= d'_{in} + d'_{ex}(t) & d''(t) &= d''_{ex}(t) \\ s'(t) &= s'_{in} + s'_{ex}(t) & s''(t) &= s''_{ex}(t) \end{aligned} \quad (4)$$

These time-dependent coefficients generally decay in a logarithmic manner during ageing, as shown in Fig. 6a.

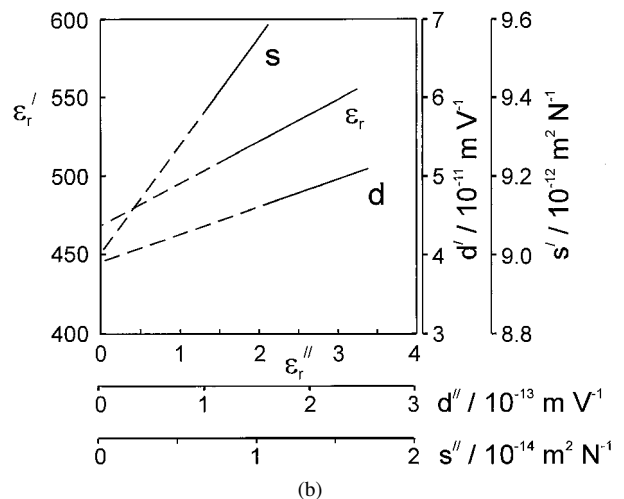
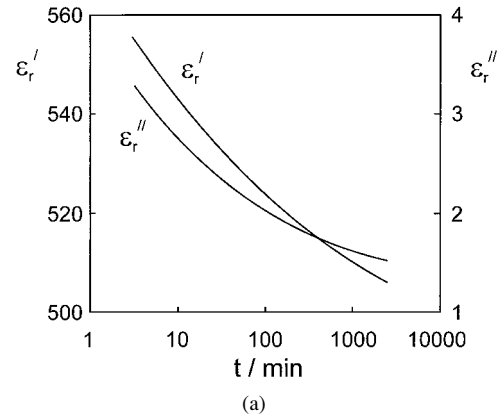


Figure 6 (a) Time dependence of ϵ_r' and ϵ_r'' , (b) $\epsilon_r' - \epsilon_r''$, $d' - d''$ and $s' - s''$ relationships for Fe doped hard PZT ceramics during ageing at 80 °C, after Herbiet *et al.* [13].

Arlt *et al.* developed a phenomenological model of a vibrating domain wall, in which it was recognised that the ratio of the imaginary to the real parts of the dielectric, piezoelectric and elastic coefficients should be constant and equal to the loss tangent $\tan \delta_{dv}$ associated with the domain wall vibration mechanism [14]:

$$\frac{\varepsilon''_{dv}}{\varepsilon'_{dv}} = \frac{d''_{dv}}{d'_{dv}} = \frac{s''_{dv}}{s'_{dv}} = \tan \delta_{dv} \quad (5)$$

Plotting the real vs imaginary components of these coefficients, measured as a function of ageing time, yielded a linear relationship with a gradient of $\tan \delta_{dv}$. Extrapolation of the line to zero loss yields the intrinsic contribution and hence enables the magnitude of the extrinsic contribution at any given ageing time to be quantified, as shown in Fig. 6b.

This separation procedure can be employed only for acceptor-doped hard ferroelectric ceramics, which exhibit significant ageing effects. The results of such measurements serve to illustrate the clamping effect of the dipolar defect associates on the domain walls and the ‘freezing out’ of the lossy domain wall contributions to the dielectric, piezoelectric and elastic properties. In particular, the substantial reduction in dielectric loss during ageing is the primary reason why acceptor-doped hard PZT ceramics can be used in low loss, high power piezoceramic components. It also accounts for the ultimate instability of hard piezoceramics under extended exposure to high AC electric fields, which can cause field-forced deageing effects that lead to large increases in dielectric loss and, eventually, transducer failure.

2.2. Dielectric nonlinearity

Early studies of dielectric nonlinearity in ferroelectric ceramics identified a ‘threshold field’ E_t , below which the dielectric properties were essentially independent of the field amplitude E_0 but beyond which both the dielectric permittivity and loss exhibited a sharp increase due to enhanced domain wall mobility or domain switching [2]. The value of E_t is often defined somewhat arbitrarily as the field amplitude at which the dielectric permittivity is observed to rise by a small fraction (say 5%) above its low-field value [15]. The threshold field level was found to be much higher in hard ferroelectrics, in comparison with soft ferroelectrics, and increased significantly during ageing [16]. Typical threshold field values are 10 V mm^{-1} for soft PZT and 300 V mm^{-1} for well-aged hard PZT [17]. Beyond E_t , the dielectric permittivity and loss were observed to increase rapidly with field amplitude due to enhanced domain wall mobility or domain switching, as shown in Fig. 7.

This behaviour represents nonlinearity in the dielectric properties, since the relative dielectric permittivity ε_r is usually defined in terms of the linear relationship between dielectric displacement D and electric field E , for which ε_r is taken to be a constant:

$$D = \varepsilon_0 \varepsilon_r E \quad (6)$$

In most practical situations, with the exception of shear mode piezoelectric transducers, the absolute permittiv-

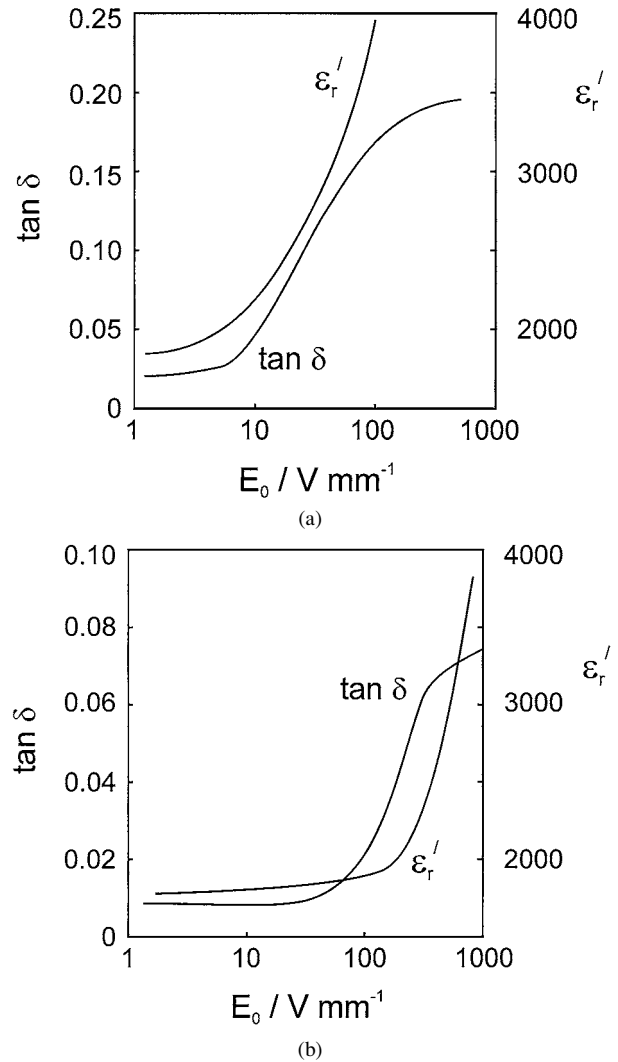


Figure 7 Dependence of dielectric permittivity and loss on field amplitude for (a) $\text{Ba}(\text{Ti}_{0.95}\text{Zr}_{0.05})\text{O}_3$ and (b) $(\text{Ba}_{0.98}\text{Ni}_{0.02})\text{TiO}_3$ ceramics, after Lewis [2].

ity given by the product $\varepsilon_0 \varepsilon_r$ is equivalent to the dielectric coefficient ε_{33} . For brevity, this coefficient is also sometimes used to represent the **relative** permittivity, as in Fig. 5 above.

The nonlinear dielectric behaviour under an alternating electric field can still be represented by an expression of the form given in Equation 6 if the relative permittivity becomes a function of field amplitude E_0 . Also, the dielectric loss that gives rise to a phase shift between D and E can be accommodated by considering ε_r as the complex quantity ε_r^* , as described above. Then, we can write:

$$D^*(t) = \varepsilon_0 \varepsilon_r^* E^*(t) \quad (7)$$

$$\text{where } E^*(t) = E_0(\cos \omega t + i \sin \omega t) = E_0 e^{i\omega t} \quad (8)$$

Most of the early studies of nonlinearity in ferroelectric ceramics focused on the value of the threshold field as a function of composition, ageing time and temperature, since this represented a boundary between near-linear behaviour at low fields and the onset of higher losses and nonlinearity at high fields. Less attention was paid to the form of the $\varepsilon_r' - E_0$ relationship or $\tan \delta - E_0$ relationship, although some of the results obtained for soft PZT ceramics appeared to show an almost linear

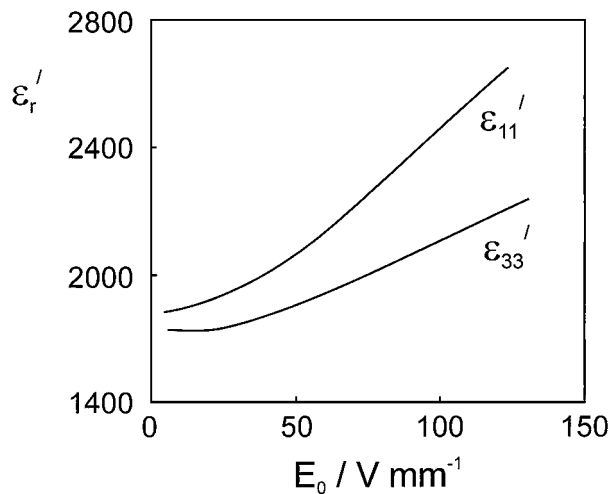


Figure 8 Electric field dependence of the dielectric coefficients ϵ_{11} and ϵ_{33} for soft PZT, after Li *et al.* [15].

increase in ϵ'_r with increasing field amplitude above E_t , as shown in Fig. 8.

Robels *et al.* demonstrated the strong dependence of the dielectric nonlinearity on doping with acceptors, for both barium titanate and PZT-based ceramics [18]. The presence of acceptor dopants reduced the nonlinear dielectric coefficients and resulted in materials that were generally more stable under high field conditions. It was found that the nonlinear behaviour for both ϵ'_r and ϵ''_r could be approximated by a polynomial function:

$$\epsilon_r(E_0) = \epsilon_r(0) + aE_0^2 - bE_0^4$$

with $a', a'', b', b'' > 0$ (9)

They also observed that for acceptor-doped ferroelectric ceramics the nonlinear coefficients all decreased significantly during ageing. Thus, it is evident that the pinning effect of the dipolar defects in acceptor-doped ferroelectrics also serves to restrain the large-scale ferroelectric domain wall motion that gives rise to nonlinearity, effectively causing a 'linearising' effect during ageing [18].

This removal of dielectric nonlinearity during ageing was also demonstrated clearly in our own studies of the P - E relationships of acceptor-doped ferroelectric ceramics in the intermediate region between the threshold field and the coercive field [19]. For example, the P - E loops given in Fig. 9 illustrate the reduction in dielectric permittivity (approximately given by the average gradient of the loop) and the almost complete removal of hysteresis and loss during ageing of a cobalt-doped BaTiO₃ ceramic at 60 °C. The corresponding ϵ'_r - t and ϵ''_r - t curves measured over a range of field amplitudes are shown in Fig. 10.

The exact form of the ϵ'_r - E_0 relationship in ferroelectric ceramics was placed under greater scrutiny during the late 1990s following studies of the direct piezoelectric effect by Damjanovic *et al.*, who demonstrated (see Section 2.3 below) a close correspondence to the classical Rayleigh Law in ferromagnetics, first reported in 1887 [20]. The Rayleigh Law applied to the dielectric properties of ferroelectric ceramics can be

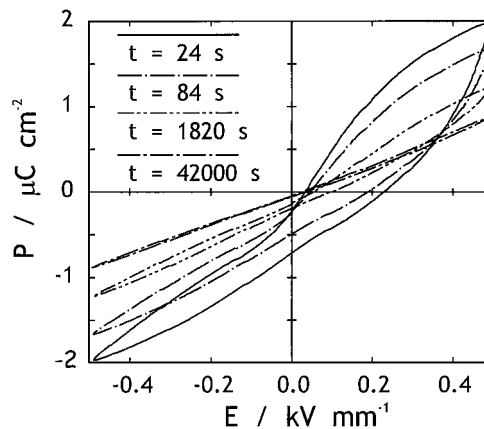
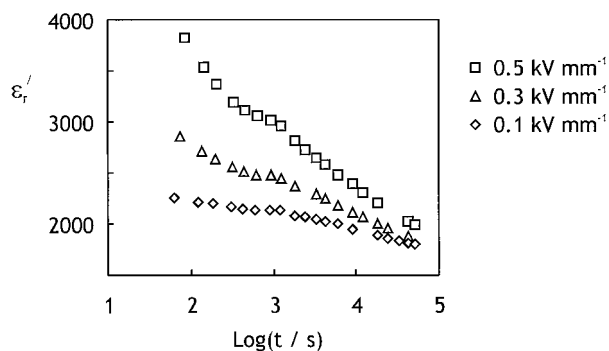
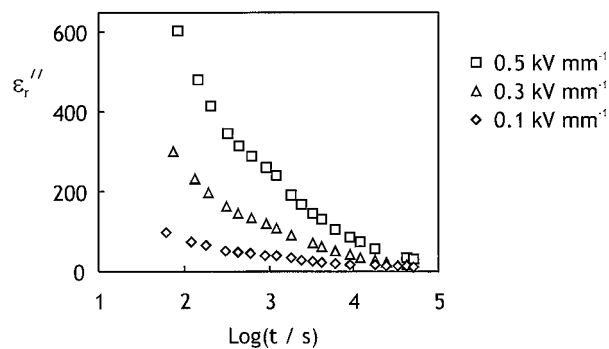


Figure 9 P - E hysteresis loops obtained for cobalt-doped BaTiO₃ ceramics during ageing at 60 °C ($E_0 = 0.5 \text{ kV mm}^{-1}$), after Hall and Ben-Omran [19].



(a)



(b)

Figure 10 Ageing of dielectric properties for cobalt-doped BaTiO₃ ceramics at 60 °C, measured at various intermediate field levels (a) ϵ'_r and (b) ϵ''_r , after Hall and Ben-Omran [19].

expressed as:

$$\epsilon'_r(E_0) = \epsilon'_r(0) + \alpha_d E_0 \quad (10)$$

and
$$D_0(E_0) = \epsilon_0(\epsilon'_r(0)E_0 + \alpha_d E_0^2) \quad (11)$$

where $\alpha_d = \text{constant}$ (dielectric Rayleigh coefficient). Here, $\epsilon'_r(0)$ is a field-independent term which is dominant at low fields and represents a combination of the intrinsic ionic response together with the contribution from reversible domain wall vibration. The term $\alpha_d E_0$ represents a contribution to ϵ'_r from larger scale irreversible domain wall translation processes, which is

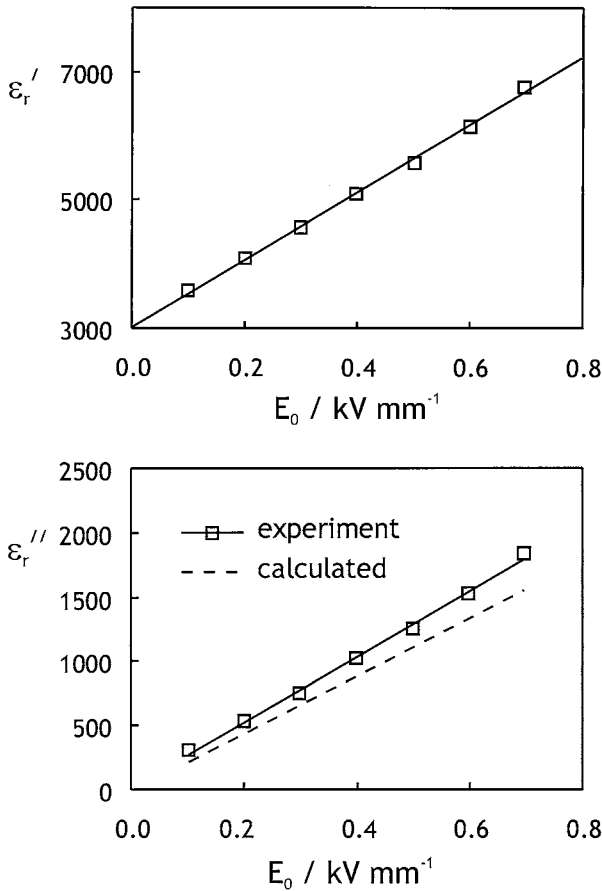


Figure 11 Field dependence of dielectric coefficients ϵ_r' and ϵ_r'' for PC5H soft PZT ($f = 20$ Hz), after Hall and Stevenson [21].

clearly dependent on the field amplitude E_0 . It was reported previously that both ϵ_r' and ϵ_r'' for soft PZT ceramics were almost linear functions of field amplitude E_0 , for $E_0 < E_c$ (where $E_c =$ coercive field), showing a good fit to expressions of the form given in equation 10. The measured relationships are shown in Fig. 11 [21].

Lord Rayleigh also made the observation that the B - H (magnetic induction-applied magnetic field) loops in the region below the coercive field could be approximated by 2 parabolic functions, the gradient of which at the loop tips was equal to the initial (low field) permeability [20]. This led to the second Rayleigh relation, which for a ferroelectric ceramic can be expressed as:

$$P = \epsilon_0([\epsilon_r'(0) + \alpha E_0]E \pm (\alpha/2)(E_0^2 - E^2)) \quad (12)$$

The expression given in Equation 12 in principle enables a simulation of the complete P - E relationship for a ferroelectric, given only 2 parameters, α and $\epsilon_r'(0)$. The simulated loops for soft PZT, constructed in this manner using the experimentally determined Rayleigh coefficient α , are shown in Fig. 12. It is clear from this figure that the simulation provides a good fit to the measured loop at $E_0 = 200$ V mm⁻¹, but there is a discrepancy between the measured and calculated data that becomes more evident with increasing E_0 . This discrepancy seems to be associated with the asymmetry of the measured P - E loops, which arises from the polar nature of the specimens.

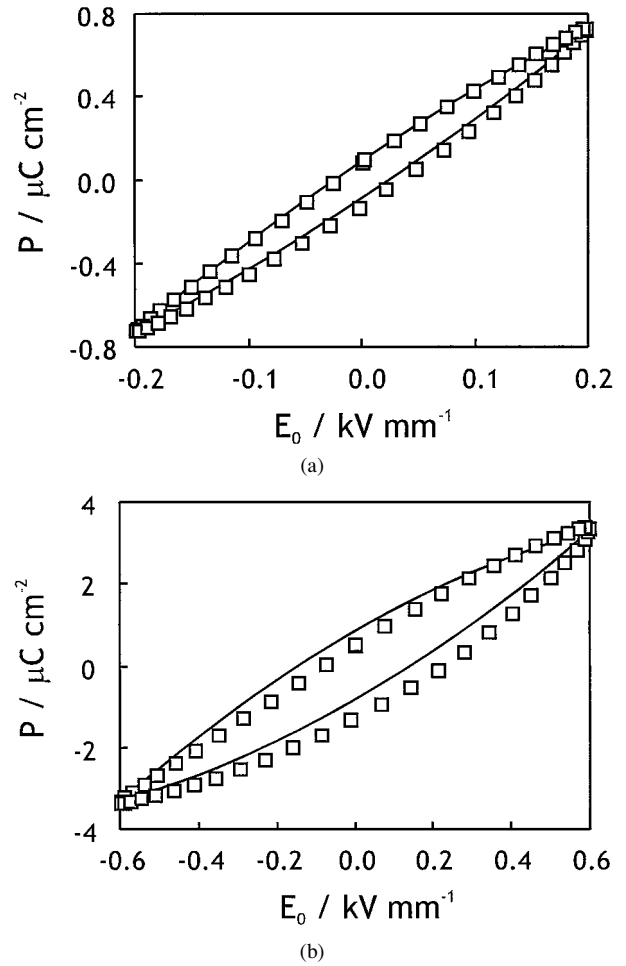


Figure 12 Comparison of calculated and experimentally determined P - E loops for PC5H at field amplitudes of (a) 0.2 kV mm⁻¹ and (b) 0.6 kV mm⁻¹, after Hall and Stevenson [21].

The second Rayleigh relationship, Equation 12, also leads to expressions for the hysteresis loss W_H and ϵ_r'' , as follows:

$$W_H(E_0) = \pi \epsilon_0 \epsilon_r'' E_0^2 \quad (13)$$

$$\epsilon_r''(E_0) = \frac{4}{3\pi} \alpha E_0 \quad (14)$$

The $\epsilon_r''(E_0)$ values calculated according to Equation 14 were all slightly less than those determined experimentally, as shown by the dashed line in Fig. 11. Nevertheless, a near-linear ϵ_r'' - E_0 relationship was still evident, but with a slightly higher gradient than expected.

At this stage, it is clear that the validity of the threshold field type of nonlinear dielectric behaviour, observed by Lewis and Hagemann amongst others [2, 16], needs to be considered in comparison with Rayleigh behaviour and the quadratic relationship described by Robels. For this reason, wide-ranging studies of the nonlinear dielectric behaviour of both soft and hard piezoceramics were carried out by the author [17, 21]. Careful attention was paid to the possible disturbing influence of continuous high field AC drive, in order to avoid complications induced by field-forced deaging phenomena.

It was found that in certain hard PZT ceramics, particularly Ferroperm types PZ26 and PZ28, a very clear

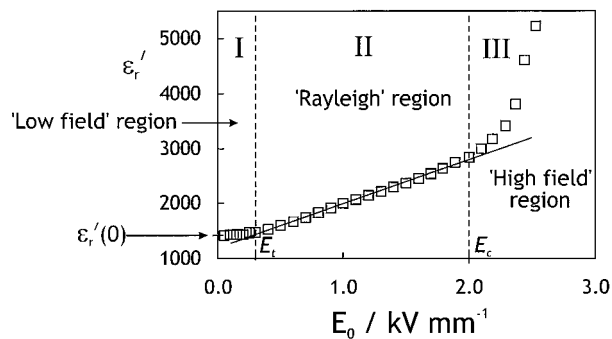


Figure 13 Schematic view of field dependence of dielectric permittivity in ferroelectric ceramics over a wide range of field strength. Data points are for Ferroperm PZ26 hard PZT ceramic, after Hall and Stevenson [21].

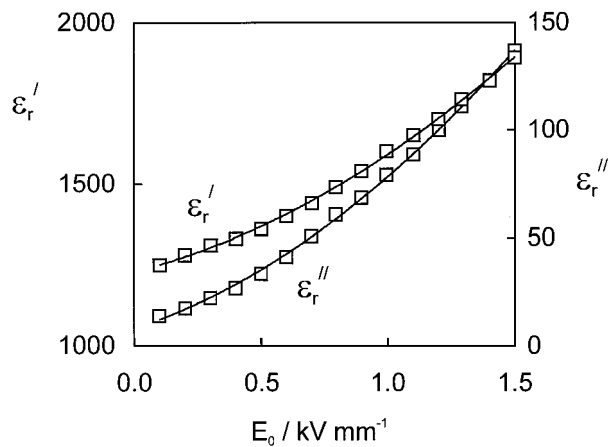
distinction could be made between a low field region (ϵ_r' almost constant), an intermediate Rayleigh region (ϵ_r' increasing proportionally to E_0), and a high field region where domain switching processes were clearly evident. The dependence of ϵ_r' on E_0 within these different regions is illustrated in Fig. 13, which incorporates some of the data obtained from measurements on PZ26 hard PZT ceramics.

It is proposed that this curve represents a general form of nonlinear dielectric behaviour that should be exhibited to a greater or lesser extent by all ferroelectric ceramics. In soft PZT, the threshold field E_t is so low that the low field region is almost indistinguishable from the Rayleigh region, unless the properties are measured very carefully over a range of field amplitudes around E_t [17].

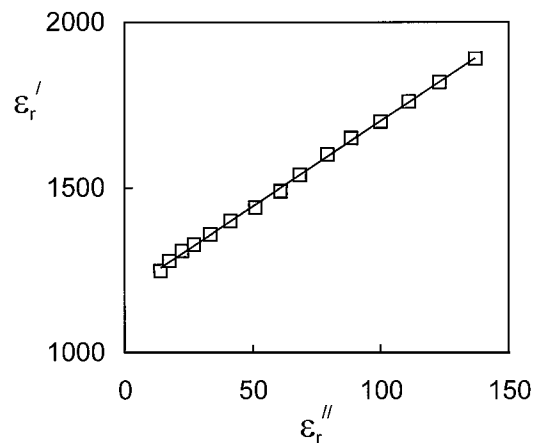
In contrast, for acceptor-doped hard ferroelectric ceramics the E_t values can be quite high ($\sim 300 \text{ V mm}^{-1}$) and under those circumstances some large-scale domain wall translation (which is thought to be the origin of Rayleigh behaviour) may occur even below E_t , giving rise to a blurring of the boundary between the low-field and Rayleigh regions. Similarly, the boundary between the Rayleigh and high field regions could also be blurred due to an overlap of domain wall translation and domain switching processes. The overall result is a smoothly varying $\epsilon_r'-E_0$ relationship with a gradually increasing slope, which yields the quadratic form described by Robels *et al.*

Finally, it is interesting to consider whether some of the concepts developed by Arlt *et al.* to describe the domain wall contributions to the low field properties of ferroelectric ceramics can be extended to the high field nonlinear regime. In particular, the direct proportionality of the domain wall contributions to the real and imaginary parts of dielectric permittivity, according to Equation 5, can be investigated by plotting the $\epsilon_r'-\epsilon_r''$ relationship, but measured as a function of field amplitude rather than ageing time.

It is found that a very good linear $\epsilon_r'-\epsilon_r''$ relationship can usually be established, as shown in Fig. 14, even when the individual $\epsilon_r'-E_0$ and $\epsilon_r''-E_0$ relationships are distinctly nonlinear. These results support the view that the slight increases in ϵ_r' and ϵ_r'' that are often observed in the low-field region can be attributed to the onset of domain wall translation and are not due to a com-



(a)



(b)

Figure 14 (a) $\epsilon_r'-E_0$, $\epsilon_r''-E_0$ and (b) $\epsilon_r'-\epsilon_r''$ relationships for Morgan Matroc PC4D hard PZT ceramic, after Hall [22].

pletely separate polarisation mechanism. A reduction in the gradient of the $\epsilon_r'-\epsilon_r''$ relationship at high fields is often observed, indicating the onset of a more lossy polarisation mechanism, which can be identified as ferroelectric domain switching [23]. Therefore, it is evident that the $\epsilon_r'-\epsilon_r''$ plot can be employed to distinguish between different lossy polarisation mechanisms.

2.3. Piezoelectric nonlinearity

Relatively few studies of nonlinearity in the piezoelectric properties of ferroelectrics were published until recently. Some earlier publications investigated the effect of a static mechanical load or an electric DC bias field on the dielectric and piezoelectric properties, as will be discussed in Section 2.6 below. Also, the generation of higher harmonic signals through dielectric or piezoelectric nonlinearity was reported by several authors (see Section 2.5). However, the effect of changing the amplitude of an applied AC pressure (for the direct piezoelectric effect) or the amplitude of the AC electric field (for the converse piezoelectric effect) received relatively little attention. This can be attributed to difficulties in measurement, since it is not straightforward to achieve a well-controlled AC pressure signal, as is required for studies of the direct piezoelectric effect. Nor is it an easy matter to accurately measure the small displacements associated with electric field-induced

strains in piezoelectric materials at sub-switching field levels.

Damjanovic and Demartin thoroughly investigated the nonlinear characteristics of the direct piezoelectric effect in ferroelectric ceramics, using a purpose-built measurement system in which a sinusoidal time-dependent stress was applied along the polar axis of certain piezoelectric ceramics [24–26]. This unique system enabled the determination of the d_{33} coefficient, through the direct piezoelectric effect, over a wide range of alternating pressure amplitude (0 to 12 MPa) and frequency (0.02 to 40 Hz). The influence of static pressure in the range 0 to 15 MPa was also investigated.

It was found in most cases that a linear increase in the d_{33} coefficient could be observed as a function of the amplitude of the applied alternating pressure X_0 , according to the following relation:

$$d_{33}(X_0) = d_{init} + \alpha_{dp} X_0 \quad (15)$$

$$\text{and} \quad Q_0(X_0) = d_{init} X_0 + \alpha_{dp} X_0^2 \quad (16)$$

where d_{init} is the initial piezoelectric charge coefficient measured at low stress, α_{dp} is the Rayleigh coefficient associated with the direct piezoelectric effect, and Q_0 is the stress induced surface charge density which is equivalent to the dielectric displacement D_0 . The non-linear component was very pronounced in some materials (e.g. soft PZT ceramic) but less so in others (e.g. strontium bismuth titanate ceramic), as shown in Fig. 15 [25].

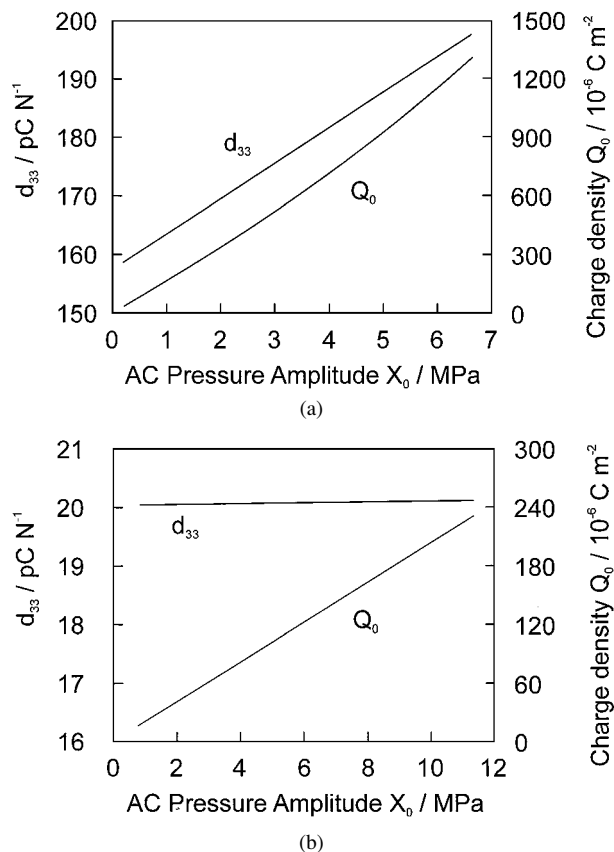


Figure 15 Piezoelectric coefficient d_{33} and piezoelectrically induced charge density Q_0 as a function of the amplitude of alternating pressure X_0 for (a) PZT and (b) strontium bismuth titanate ceramics, after Damjanovic and Demartin [25].

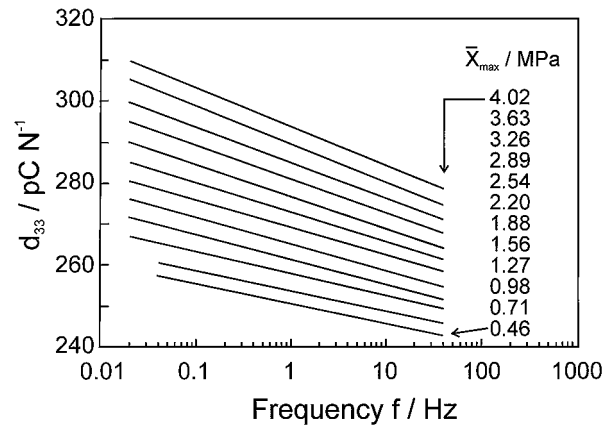


Figure 16 The longitudinal d_{33} piezoelectric coefficient of soft PZT ceramic as a function of the frequency of the alternating pressure, at different amplitudes of the average alternating pressure \bar{X}_{max} , after Damjanovic [27].

The hysteretic Q - X (charge-stress) relationship showed a close correspondence to Rayleigh's second relationship, which for the direct piezoelectric effect can be expressed as:

$$Q = (d_{init} + \alpha_{dp} X_0) X \pm (\alpha_{dp} / 2) (X_0^2 - X^2) \quad (17)$$

By analogy with the Rayleigh Law in ferromagnetics, the authors concluded that the stress-dependent term $\alpha_{dp} X_0$ was due to a mechanism involving the translation of non-180° ferroelectric domain walls (90° for tetragonal or 71/109° for rhombohedral ceramics) across an array of pinning defects. It was recognised by Damjanovic that a hysteretic domain wall translation mechanism involving interaction of the moving domain wall with pinning centres should also result in a logarithmic dependence of the dielectric permittivity or piezoelectric coefficient on frequency f , as shown in Fig. 16 [27].

By analysing the stress and frequency dependence of d_{33} , it was demonstrated that both the reversible d_{init} and irreversible $\alpha_{dp} X_0$ contributions to d_{33} were frequency dependent, according to the following relationships:

$$d_{init}(\omega) = d_0 + d \ln(1/\omega) \quad (18)$$

$$\alpha(\omega) = a_0 + a \ln(1/\omega) \quad (19)$$

More general relationships were also derived to describe the dependence of d_{33} on both ω and X_0 :

$$d_{33}(\omega, X_0) = G_0(X_0) + G(X_0) \ln(1/\omega) \quad (20)$$

$$\text{with} \quad G_0(X_0) = g_0 + f_0 X_0 \quad (21)$$

$$\text{and} \quad G(X_0) = g + f X_0 \quad (22)$$

Using this method, it was possible to develop a numerical model for the direct piezoelectric effect, involving just 4 fitting parameters. The values of these constants for a soft PZT ceramic were found to be $g_0 = 249$ pC N⁻¹, $f_0 = 13.2$ pC N⁻¹ MPa⁻¹, $g = 1.8$ pC N⁻¹ and $f = 0.59$ pC N⁻¹ MPa⁻¹. A similar approach could be adopted to describe the dielectric behaviour and/or the converse piezoelectric effect in ferroelectrics,

provided that an analogous field and frequency dependence of the relevant dielectric and piezoelectric coefficients could be demonstrated. However, it should be noted that the effect of simultaneous variations in stress and electric field have not yet been considered.

Sherrit *et al.* observed qualitatively similar variations in the d_{33} coefficient of soft PZT ceramics, measured through the direct piezoelectric effect, as functions of the amplitude and frequency of the applied stress [28]. In their case, a quasistatic measurement method was employed in which a gradually increasing or step stress was applied along the polar axis of Channel 5804 PZT. The measured d_{33} value was observed to increase from around 200 to 430 pC N⁻¹ as the stress increased from 0 to 70 MPa. The time-dependence of the domain switching process was observed as a logarithmic decay of the depolarisation current. Sherrit *et al.* also observed a strong temperature dependence of d_{33} , which was fitted to an Arrhenius relation with an activation energy in the range 0.2 to 0.7 eV, depending on the material.

Nonlinearity in the converse piezoelectric effect has been reported in several recent publications [29–32]. Mueller *et al.* investigated the nonlinear dielectric and piezoelectric behaviour of soft PZT ceramics, finding that the experimental data could be described using a power law relationship [29, 30]:

$$m(E_0) = m_0 + A[(E_0 - E_t)/E_t]^\phi \quad (23)$$

where m is a dielectric or piezoelectric coefficient, E_t is a threshold field, and ϕ is an exponent. The value of ϕ for a soft PZT ceramic was found to be approximately 1, corresponding to the Rayleigh Law, when the electric field was parallel to the polar axis (i.e. for ϵ_{33} and d_{33}). In contrast, a value of $\phi \approx 1.2$ was found for ϵ_{11} and d_{15} from measurements made using shear-mode piezoelectric devices. The results obtained for the dielectric and piezoelectric coefficients showed a good fit to the power law, as shown in Fig. 17.

It was also noted by Mueller that the lossy imaginary components of ϵ and d could be represented by similar power law expressions. Furthermore, the ratio of the imaginary to the real parts of the nonlinear coefficients remained approximately constant as a function of increasing field amplitude. The corresponding $\epsilon' - \epsilon''$ or $d' - d''$ plot should be linear, as was noted above (Fig. 14).

Kugel and Cross observed a linear dependence of ϵ_{33} and d_{31} on field amplitude E_0 for various soft PZT ceramics [31]. A striking correspondence was noted between the field-dependent dielectric and piezoelectric coefficients, as shown in Fig. 18, indicating their common origin in 90° ferroelectric domain wall translation. A similar linear dependence of ϵ_{33} , d_{33} and d_{31} on field amplitude was also noted by Sherrit *et al.* [32].

The resulting Rayleigh Law for the converse piezoelectric effect can be written as:

$$d(E_0) = d_{init} + \alpha_{cp} E_0 \quad (24)$$

$$\text{and} \quad X_0(E_0) = d_{init} E_0 + \alpha_{cp} E_0^2 \quad (25)$$

The direct proportionality between field-induced displacement D and strain x was also evident in the

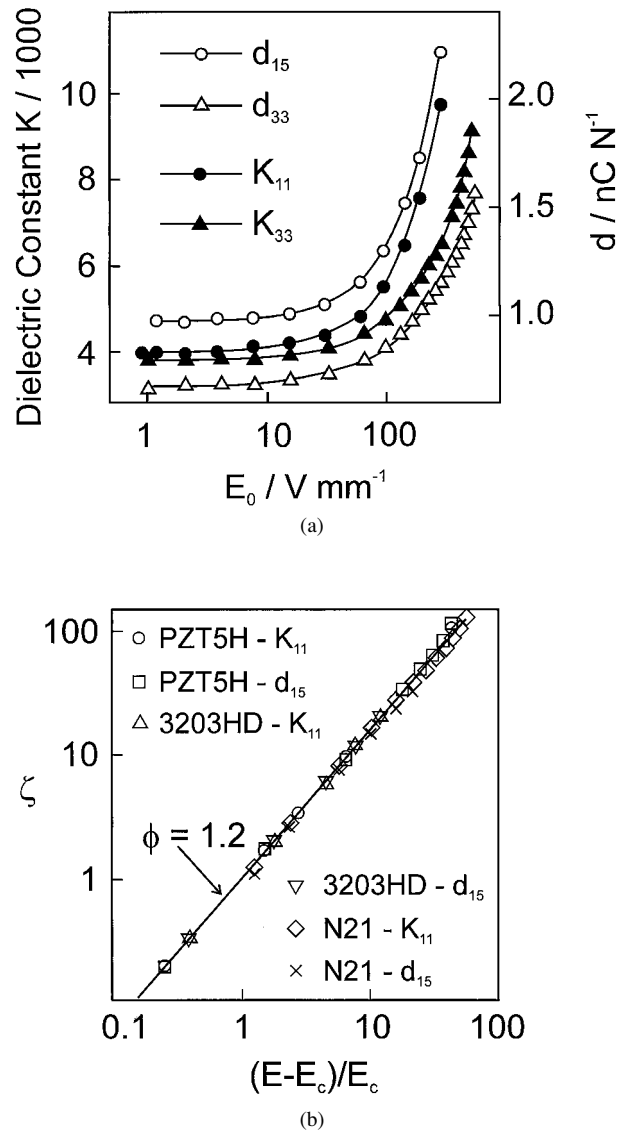


Figure 17 (a) AC field dependence of dielectric and piezoelectric coefficients of soft PZT ceramic (b) data fitted to power law relationship according to Equation 23, after Mueller and Zhang [30].

x - D relation reported by Kugel and Cross, which remained linear even when the individual x - E and D - E relationships were distinctly nonlinear and hysteretic. These results indicate that the nonlinear piezoelectric coefficients could potentially be derived from the nonlinear dielectric coefficients, providing a possible means of reducing the number of parameters required to describe the nonlinear dielectric and piezoelectric behaviour.

2.4. Elastic (mechanical) nonlinearity

Nonlinearity in the elastic properties of ferroelectric ceramics has received relatively little attention, particularly for applied stresses in the range below that required to cause irreversible depoling, sometimes referred to as the coercive stress X_c . Early studies demonstrated that a compressive stress applied parallel to the polar axis could induce a degradation of the dielectric and piezoelectric properties, due to ferroelastic domain rearrangement [33]. The sensitivity to stresses applied in a direction perpendicular to the polar axis was

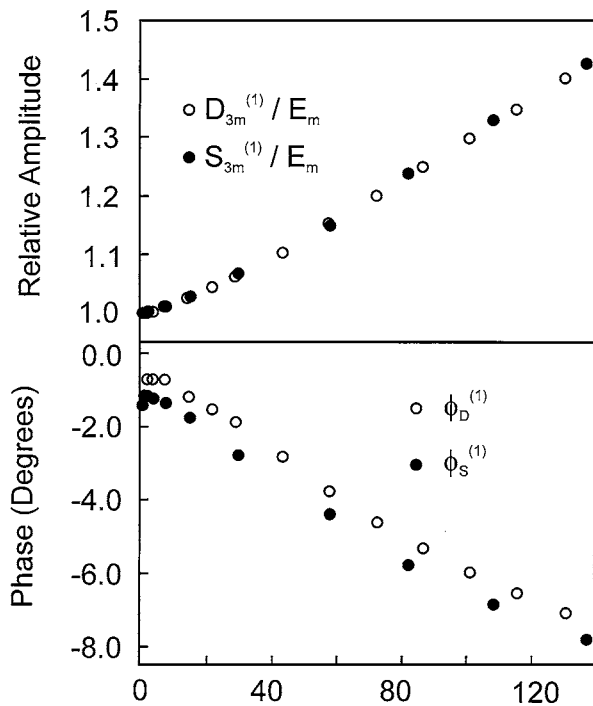


Figure 18 Relative field dependencies of ϵ_{33} and d_{31} , derived from the amplitudes of the fundamental harmonic components of the dielectric displacement and strain signals, for 3203 HD soft PZT ceramic at 100 Hz, after Kugel and Cross [31].

significantly smaller, presumably because the degree of stress-induced domain reorientation was less [34].

The development and commercial application of piezoelectric actuators has led to a renewed interest in nonlinearity in the elastic properties of piezoelectric ceramics. It is recognised that both residual and field-induced stresses in multilayer actuators play a deciding role in the fatigue characteristics and ultimate lifetime of practical devices. Cao and Evans carried out a detailed study of elastic nonlinearity in a range of ferroelectric (piezoelectric), relaxor ferroelectric (electrostrictive) and antiferroelectric (phase change) ceramics [35]. It was observed that the elastic properties of both soft and hard PZT ceramics were distinctly nonlinear when the applied compressive stress exceeded a level ~ 20 MPa, as shown in Fig. 19. A permanent change in strain on removal of the load was readily apparent in soft PZT ceramics, due to irreversible ferroelastic domain switching. Hard PZT ceramics showed a more complete strain recovery, but a permanent deformation became evident for stresses exceeding 200 MPa.

It was found that the results obtained for the deviatoric plastic strain x'_p could be described in terms of a power law expression, which was similar to that observed in other ceramic systems exhibiting phase transformation behaviour:

$$X'/X'_0 = (x'_p/x'_0)^a + (x'_p/x'_0)^b \quad (26)$$

where a and b are empirical power law coefficients, $a < 1$ and $b > 1$, X'_0 is a reference stress and x'_0 is a reference strain.

The mechanical depolarisation behaviour of the specimens, measured by means of the electric charge released on application of the stress, gave a close corre-

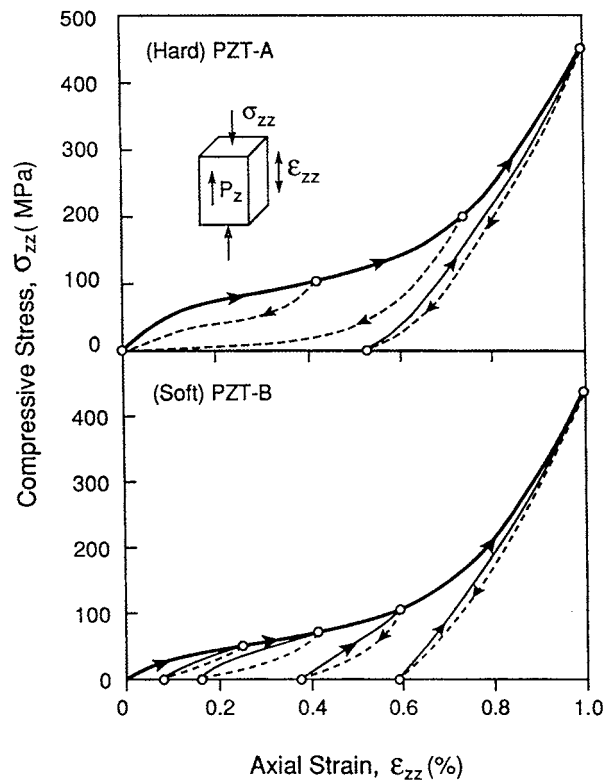


Figure 19 Stress-strain curves for soft and hard PZT ceramics subjected to stress along the polar axis, after Cao and Evans [35].

spondence to the purely elastic results. Thus, it was confirmed that the observed elastic nonlinearity could be attributed to the reorientation of ferroelectric-ferroelastic domains.

The origin of the 'memory' effect in hard PZT ceramics, in which the original state of strain and of polarisation could be recovered even after a high degree of mechanical depolarisation, was not explained by Cao and Evans. Subsequently, Schäufele and Härdtl recognised that this effect was most likely associated with the presence of oriented dipolar defect associates in the hard PZT ceramics, which were relatively unaffected by the mechanical domain rearrangement process for short term loading/unloading experiments [36]. The position and orientation of these defects facilitates the recovery of the original domain configuration, provided that the duration of the loading/unloading experiment is short relative to the relaxation time τ of the dipolar defects. The ferroelectric domain and dipolar reorientation processes for a hard PZT ceramic due to stresses applied along the polar axis are illustrated schematically in Fig. 20.

It was confirmed that the remanent strain and depolarisation in hard PZT ceramics were strongly dependent on both the maximum applied stress and the duration of the loading experiment. For example, for a hard PZT ceramic subjected to a load of 400 MPa the remanent strain and polarisation obtained for a compression time of 3600 s (5.3×10^{-3} and 323 mC m^{-2} respectively), were more than an order of magnitude greater than those obtained for 1 s (0.3×10^{-3} and 10 mC m^{-2} respectively).

The time dependence of mechanical depolarisation in ferroelectric ceramics was investigated further by

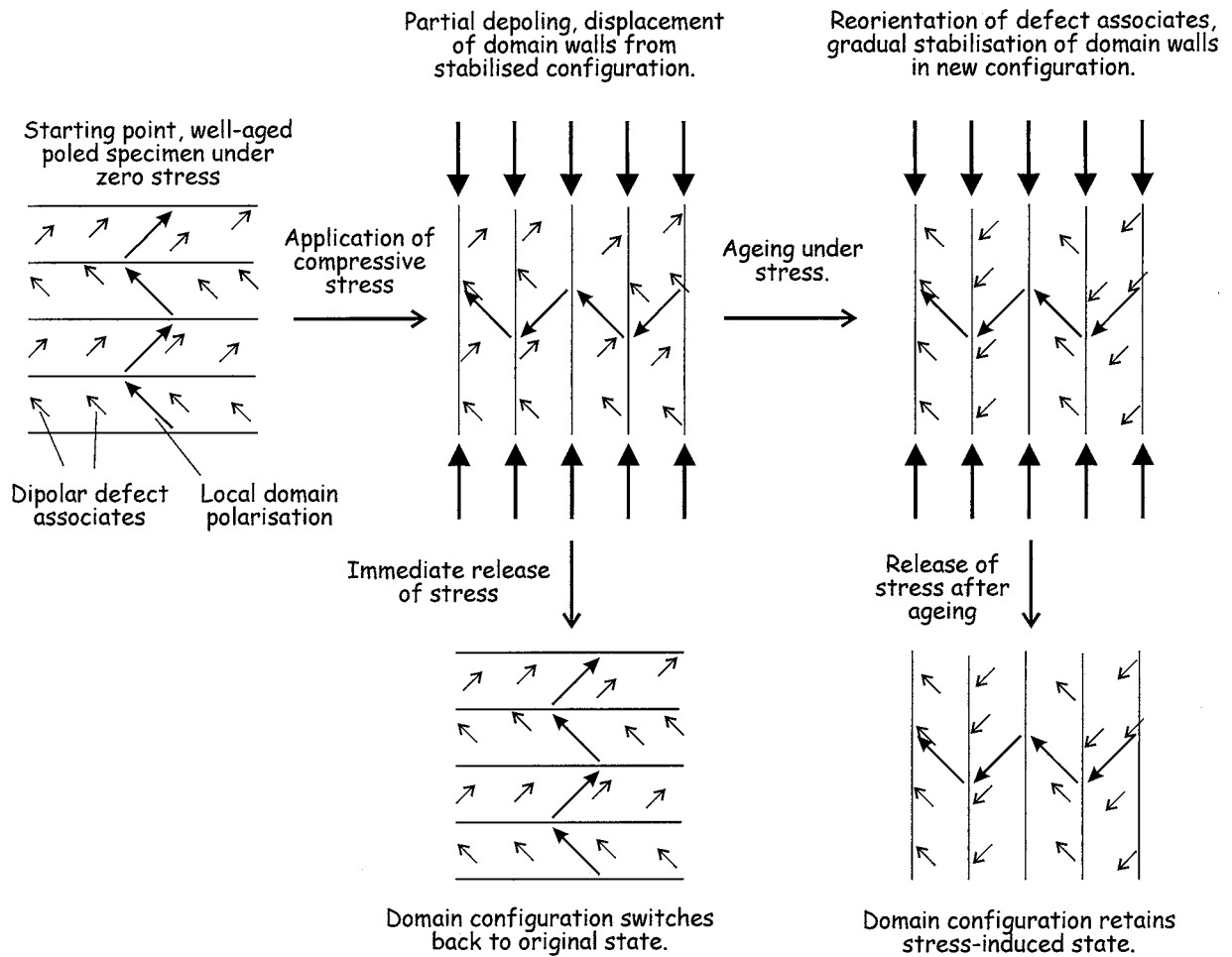


Figure 20 Schematic illustration of time-dependent ferroelectric domain and dipolar reorientation processes in hard PZT due to stress applied along the polar axis.

Heilig and Härdtl, who demonstrated that the charge released in response to a step function load increased in a logarithmic manner with time under stress [37]. The following empirical function was used to describe this behaviour:

$$Q(t) = Q_i + Q_0(t/t_0)^\alpha \quad (27)$$

The resulting charge-time curves for a soft PZT ceramic are illustrated in Fig. 21. It was supposed that this gradual release of charge was characteristic of a time dependent ferroelectric domain switching or domain wall translation process.

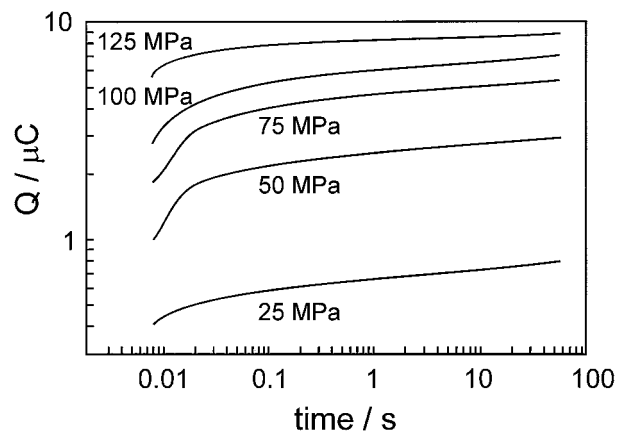


Figure 21 Response of the charge on stress steps for soft PZT, after Heilig and Härdtl [37].

The response time of this effect spanned the range from 0.01 s (the resolution of the apparatus) to at least 100 s, which was noted to be several orders of magnitude larger than the domain switching times of the order of a few μs or less that had previously been reported for the switching of individual domains in ferroelectric single crystals or thin films. However, it can be noted that the response times measured by Heilig and Härdtl [37] are of the same order of magnitude as those associated with the domain wall translation process described by Damjanovic [27].

The influence of the ceramic composition, in terms of the Zr concentration in PZT, and the presence of an electric bias field on the elastic nonlinearity were also reported by Schäufele and Härdtl [36]. It was shown that both the coercive stress X_c and the coercive field E_c reduced as a function of increasing Zr concentration, exhibiting minimum values near the morphotropic phase boundary ($\sim 56\%$ Zr). It was also confirmed that an electric bias field applied parallel to the polar axis acted to stabilise the state of remanent polarisation, resulting in an increase in the coercive stress X_c . The dependence of X_c on the bias field E_b yielded a near-linear relationship, as shown in Fig. 22, which could be explained on the basis of the energy density required to initiate ferroelectric domain switching w_{ds} :

$$X_c x + E_b(-\Delta P) = w_{ds} \quad (28)$$

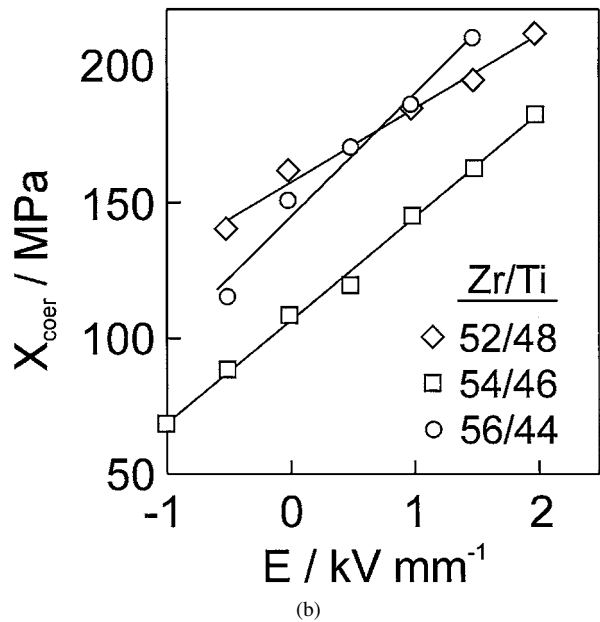
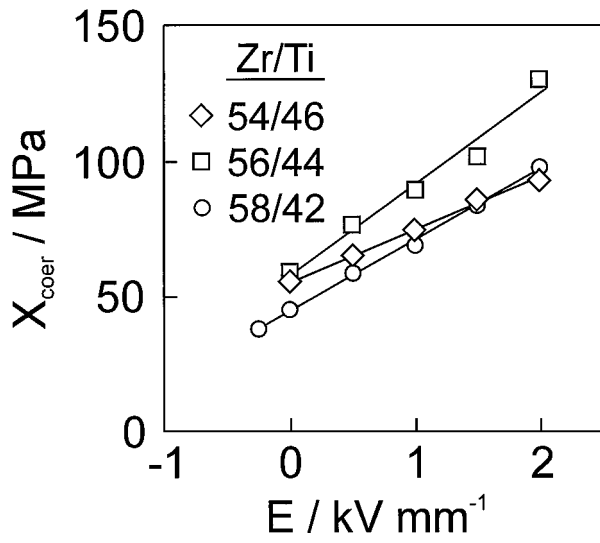


Figure 22 Linear dependence of coercive stress on electric field applied to (a) soft and (b) hard PZT with different Zr concentrations (for soft PZT: $\diamond = 0.54$ $\square = 0.56$ $\circ = 0.58$, for hard PZT: $x = 0.52$ $*$ $= 0.54$ $+ = 0.56$), after Schäufele and Härdtl [36].

where x = strain and ΔP = the change in polarisation associated with domain switching. Rearrangement of this equation yields a linear relationship between X_c and E_b with slope $\Delta P/x$:

$$X_c = \frac{\Delta P}{x} E_b + \frac{w_{ds}}{x} \quad (29)$$

A qualitative agreement was established between the ratio $\Delta P/x$ measured from the gradient of the X_c - E_b curve and the values of remanent depolarisation and strain measured directly from the stress-strain and stress-depolarisation curves.

2.5. Harmonic generation through nonlinear dielectric and piezoelectric properties

The nonlinear nature of the dielectric and piezoelectric properties of ferroelectric ceramics often becomes evident through the generation of higher-order electric current or strain/displacement signals from a pure

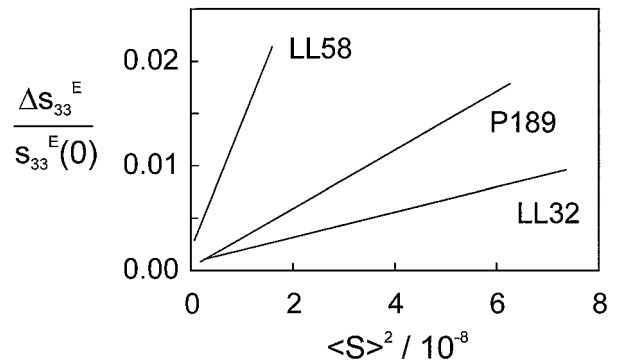


Figure 23 Change of mechanical compliance s_{33} for various PZT ceramics as a function of the mean squared strain, after Gonnard *et al.* [39].

sinusoidal time dependent electric field $E = E_0 \sin(\omega t)$. This effect is particularly important for acoustic piezoelectric transducers operating close to resonance (or antiresonance), since a significant proportion of the electrical input energy can be wasted in the generation of unwanted vibrational modes [38]. Fourier analysis techniques can be used to detect the harmonic components of the output signal and subsequently to relate their magnitude, phase and frequency to the nonlinear material coefficients.

Gonnard *et al.* used this method to determine the high power resonance characteristics of hard PZT longitudinal piezoelectric resonators [39]. By combining the electrical impedance characteristics measured around the resonance with a nonlinear model of a piezoelectric resonator, it was possible to derive the change in elastic compliance s_{33} as a function of strain, as shown in Fig. 23.

The generation of higher order harmonic signals in the time dependent field-induced strain and dielectric displacement waveforms was also analysed by Kugel and Cross, who studied the longitudinal dielectric displacement D_3 and the transverse strain x_1 of soft PZT ceramics in a bimorph cantilever configuration [31]. Under stress-free conditions, the nonlinear dielectric and piezoelectric relations were expressed as:

$$D_3 = \varepsilon_{33}^X E + \varepsilon_{333}^X E^2 + \varepsilon_{3333}^X E^3 + \dots \quad (30)$$

$$x_1 = d_{31} E + R_{331} E^2 + R_{3331} E^3 + \dots \quad (31)$$

At first sight, it might appear that these equations have the same form as the Rayleigh Law, given above in equations 10 and 25, although extending to higher order terms in E . However, it is important to recognise that this is not the case since these equations, which are derived from the thermodynamic approach (see Section 3 below) relate the instantaneous displacement or strain (D , x) to the instantaneous electric field E . In contrast, the Rayleigh Law expresses the relationship between the **amplitude** of the displacement or strain waveform (D_0 , x_0) and that of the electric field waveform E_0 . It is shown below that the amplitudes and phases of the harmonic components derived from the second Rayleigh relation are very different to those found from the thermodynamic relations.

By substituting the time dependent expression for E into Equations 30 and 31, the Fourier components of

the dielectric displacement D_3 and strain x_1 waveforms can be found as:

$$D_3^{(1)} = \left(\varepsilon_{33}^x + \frac{3}{4} \varepsilon_{3333}^x E_0^2 + \dots \right) E_0 \sin(\omega t) \quad (32)$$

$$D_3^{(2)} = \left(\frac{1}{2} \varepsilon_{3333}^x E_0 + \dots \right) E_0 \sin\left(2\omega t - \frac{\pi}{2}\right) \\ \rightarrow D_3^{(2)} = \left(\frac{1}{2} \varepsilon_{3333}^x E_0 + \dots \right) E_0 \sin\left(2\omega t - \frac{\pi}{2}\right) \quad (33)$$

$$D_3^{(3)} = \left(\frac{1}{4} \varepsilon_{3333}^x E_0^2 + \dots \right) E_0 \sin(3\omega t - \pi) \quad (34)$$

$$X_1^{(1)} = \left(d_{31} + \frac{3}{4} R_{3331} E_0^2 + \dots \right) E_0 \sin(\omega t) \quad (35)$$

$$X_1^{(2)} = \left(\frac{1}{2} R_{331} E_0 + \dots \right) E_0 \sin\left(2\omega t - \frac{\pi}{2}\right) \quad (36)$$

$$X_1^{(3)} = \left(\frac{1}{4} R_{3331} E_0^2 + \dots \right) E_0 \sin(3\omega t - \pi) \quad (37)$$

These equations are derived in a straightforward manner by considering the expansions of $\sin^2(\omega t)$ and $\sin^3(\omega t)$ in terms of $\sin(2\omega t)$ and $\sin(3\omega t)$ respectively. It is apparent from Equations 32 and 35 that, according to this approach, the fundamental components of ε_{33} and d_{31} should exhibit a dependence on the square of the electric field amplitude E_0^2 , whereas the Rayleigh Law describes a dependence on E_0 . Kugel and Cross demonstrated that these equations, derived from the thermodynamic theory, gave a very poor fit to the experimental data [31].

For this reason, an alternative approach was proposed based on a hysteretic model of the D - E and x - E relationships. This led to more complex expressions for the magnitudes of the harmonic components of x and D , but gave a much better fit to the experimental data, as shown in Fig. 24. The authors concluded that such a hysteretic model was necessary to describe the ob-

served results and that a polynomial function of the form given in Equations 30 and 31 was clearly inadequate. The hysteretic model developed by Kugel and Cross was found to reduce to Rayleigh's second relationship, Equation 12, when higher order terms were omitted [31].

Ishii *et al.* carried out a study of harmonic generation in which the drive current in a piezoelectric transducer was controlled to provide a pure sinusoidal current density, $J = J_0 \sin(\omega t)$ [40]. In this case, material nonlinearities led to the generation of harmonic voltage signals, explained according to the following polynomial relation:

$$E = -hx + \beta'' J + \gamma' J^2 + \xi' J^3 \quad (38)$$

where h is a piezoelectric voltage coefficient and β'' , γ' and ξ' are constants related to the linear and nonlinear dielectric coefficients. The use of this relationship appeared to provide a good fit to the experimental data.

2.6. The influence of static electric and elastic fields on nonlinearity

Numerous studies have been carried out to determine the influence of electric bias fields and static stress on the dielectric properties of ferroelectrics. The results of such investigations are often interpreted in terms of phenomenological thermodynamic theories of ferroelectric phase transformations [41–43]. These usually provide a good understanding of the observed phenomena, including the change in dielectric permittivity or ferroelectric Curie temperature with increasing stress or electric field. The influence of a static electric or elastic field on the nonlinear properties of ferroelectric ceramics is less well characterised or understood. A diverse range of behaviour can be observed, depending on the composition/structure of the material under investigation, the orientation of the applied field with respect to the polar axis (positive or negative bias), and the time scale over which the field is applied or removed.

Butler and Rolt summarised the practical consequences of combined static stress and alternating electric drive on the operating characteristics of high power SONAR transducers, with particular emphasis on hard PZT ceramics [44]. They concluded that operation at field amplitudes up to 800 V mm^{-1} and compressive stresses of 100 MPa were achievable in practical transducers. Higher levels of stress or AC field would inevitably lead to unacceptable changes in the transducer properties (degradation of piezoelectric activity, detuning, high dielectric losses etc.).

One of the first detailed studies of the effects of static compressive stress on the properties of PZT ceramics was reported by Krueger [33]. It was found that repeated cycling of hard PZT ceramics at stresses $\sim 100 \text{ MPa}$ led to a partial but permanent depolarising effect, with a consequent reduction in the d_{33} coefficient. The dielectric permittivity measured at both low and high electric field levels increased significantly on the application of stress, as shown in Fig. 25a. The increase in the loss tangent was even more dramatic, causing some concern over potential heat generation in high power transducers. It was noted by Krueger that the apparent high $\tan \delta$ value was most likely due to the 'deageing' effect

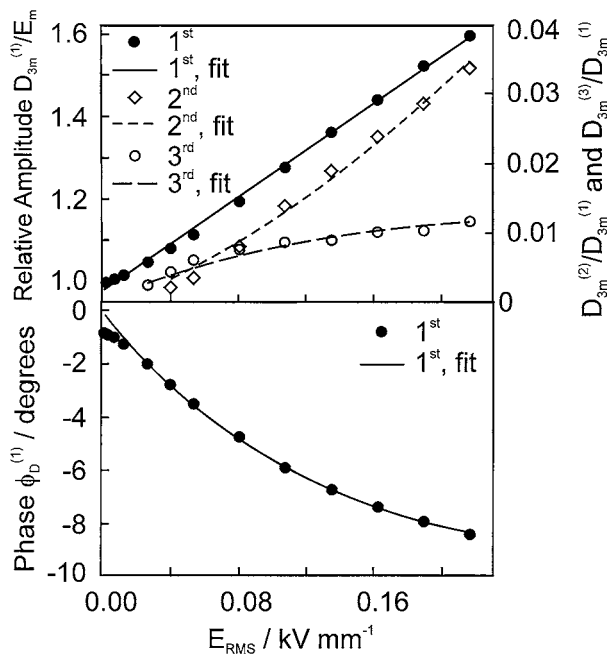


Figure 24 Results of fitting the hysteretic model to experimental data for the amplitudes of the first 3 harmonics of D_3 for 3203HD soft PZT ceramic, after Kugel and Cross [31].

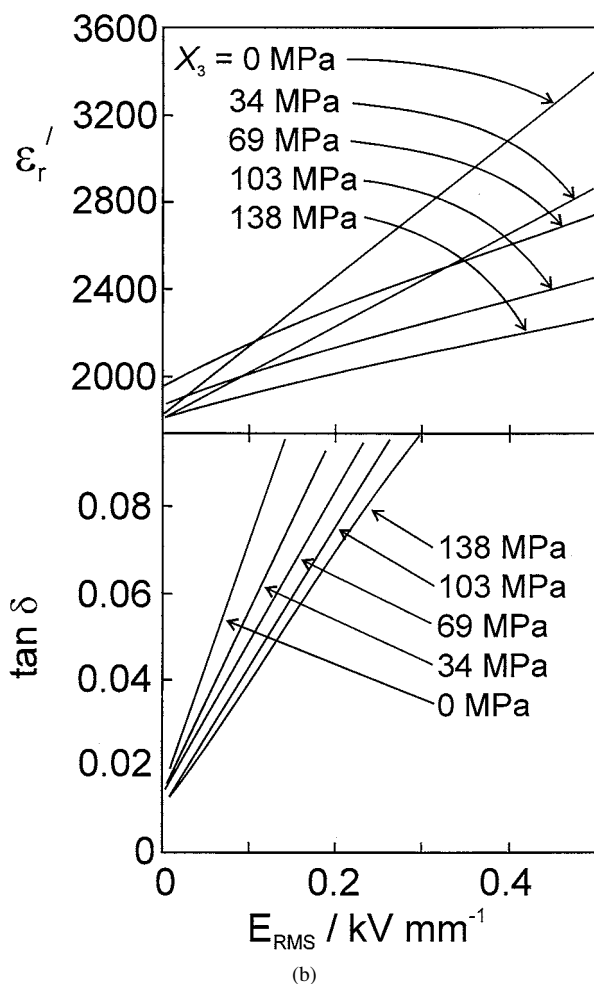
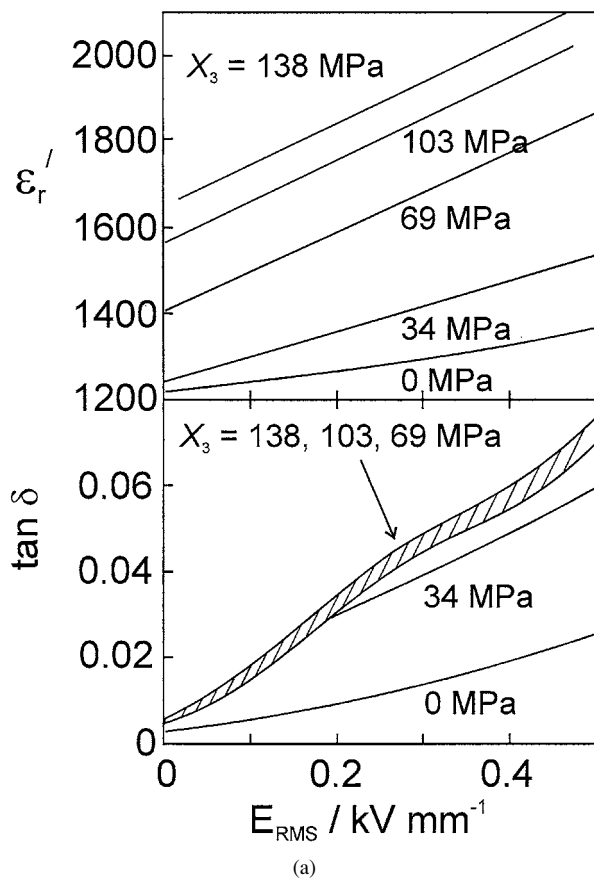


Figure 25 The effect of static stress and alternating electric drive field on the dielectric properties of (a) hard and (b) soft PZT ceramics, after Krueger [33].

of the applied stress and that subsequent ageing under stress should lead to improved $\tan \delta - E_0$ characteristics. This also served to highlight the fact that exposure to any large mechanical, electrical or thermal disturbance in service could cause a similar increase in $\tan \delta$.

The effect of stress on the high field dielectric properties of a soft PZT ceramic was also reported as shown in Fig. 25b. In this case, a drastic reduction in d_{33} was observed above a stress ~ 30 MPa, indicating the occurrence of a permanent depolarisation process. The high field dielectric measurements on soft PZT ceramics showed a significantly greater sensitivity to field amplitude, but the applied stress gave rise to a **reduction** in both ϵ_r and $\tan \delta$ (as opposed to the increase noted for hard PZT). Clearly, the domain pinning effects in soft PZT ceramics are much weaker than those in hard PZT, with the result that the stress-induced deageing effect does not seem to be significant. Instead, the applied stress appears to act to reduce the ferroelectric domain wall mobility, resulting in a marked reduction in the gradient of the $\epsilon_r - E_0$ and $\tan \delta - E_0$ curves.

Krueger also made the important practical point that the thin disks required for the high field measurements were not well suited for the application of a pure axial compressive stress, since lateral clamping would inevitably result in opposing radial stresses and hence introduce a large hydrostatic component. Therefore, in certain other investigations where thin disk specimens have been employed for high field measurements under a nominal uniaxial stress, the possible presence of a significant hydrostatic component should not be discounted.

The stress-induced deageing effect in hard acceptor-doped PZT ceramics has also been described in several recent publications [45–47]. In our own work, it was found that both the dielectric permittivity and loss of a hard PZT ceramic increased significantly on the application of a compressive stress, but that ageing under stress led to logarithmic reductions in ϵ_r' and ϵ_r'' with time, as shown in Fig. 26 [46]. Comparable increases in ϵ_r' and ϵ_r'' were observed on removal of the stress, which can also be interpreted in terms of a stress-induced deageing effect caused by the rearrangement of ferroelectric domains relative to a fixed array of dipolar defects, as illustrated in Fig. 20 above.

The field dependence of permittivity and loss under stress showed a very similar form to that described by Krueger (Fig. 25). Further analysis of the data, in terms of the $\epsilon_r' - \epsilon_r''$ relationship obtained as a function of field amplitude (Fig. 27) indicated that the low field permittivity of these hard PZT ceramics (obtained by extrapolation to zero loss) did increase significantly under stress.

A complete explanation of the differing behaviour of soft and hard PZT ceramics under stress has not yet been presented, although it is clear that the arguments must include consideration of the effects of stress on the intrinsic ionic polarisation mechanism, as well as those due to reversible and irreversible ferroelectric domain wall motion [45–47]. The influence of residual (intergranular) stress should also be accounted for, as was discussed by Damjanovic and Demartin [24, 26]. They

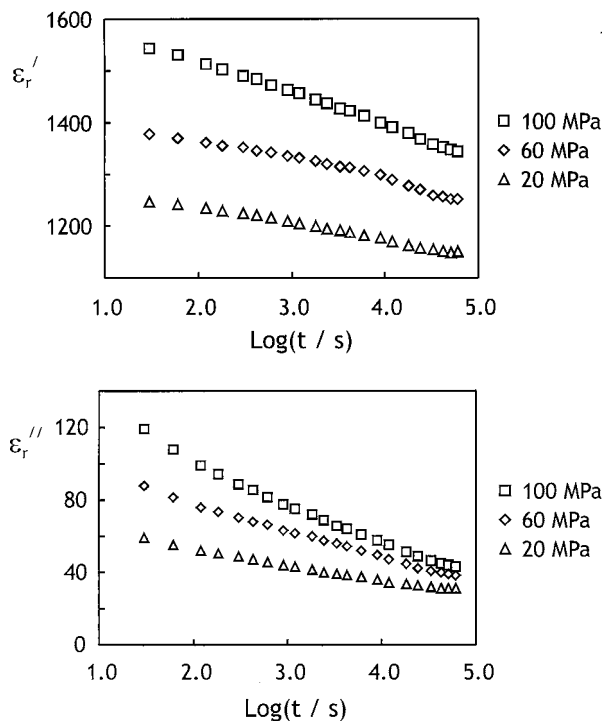


Figure 26 Variation in high field dielectric coefficients of PC8 hard PZT ceramics during ageing under various levels of applied compressive stress ($E_0 = 1 \text{ kV mm}^{-1}$), after Hall *et al.* [46].

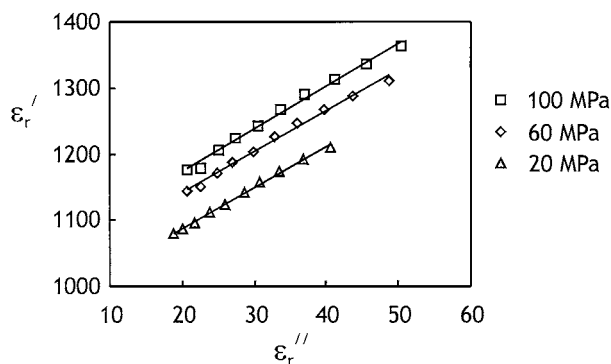


Figure 27 $\epsilon_r' - \epsilon_r''$ plots obtained as a function of field amplitude at various applied stresses for PC8 hard PZT ceramics ($E_0 = 1 \text{ kV mm}^{-1}$, ageing time = 20 hours), after Hall *et al.* [46].

noted in their work on the direct piezoelectric effect in barium titanate and PZT ceramics that a superimposed bias pressure led to an increase in the ‘threshold pressure’ required to initiate domain wall motion and a reduction in the Rayleigh coefficient α_{dp} , representing the gradient of the $d_{33} - X_0$ relationship (Fig. 28). This indicates that the application of a static pressure tends to inhibit the domain wall contributions to the piezoelectric coefficient, in common with the effects noted above for the dielectric properties.

Furthermore, it was found that the influence of the static pressure was much less pronounced for tetragonal PZT (in comparison with rhombohedral PZT) and for fine-grained barium titanate (in comparison with coarse-grained barium titanate). The results were explained in terms of the presence of a higher residual stress in the tetragonal PZT and fine-grained barium titanate ceramics, resulting from the paraelectric-

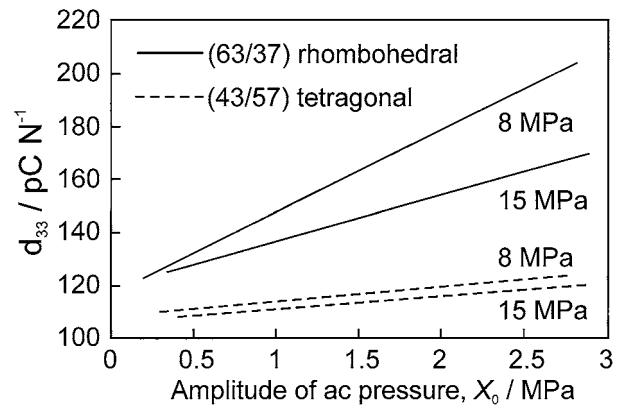


Figure 28 d_{33} as a function of the amplitude of ac pressure for rhombohedral (63/37) and tetragonal PZT ceramics doped with 4 at% Nb at 8 and 15 MPa dc pressure, after Damjanovic and Demartin [26].

ferroelectric phase transformation. This residual stress acts to restrict the ferroelectric domain wall motion in such materials, since domain wall movement requires a further increase in elastic energy. The application of an external static pressure will certainly cause a further reduction in domain wall mobility, but to a lesser extent than would be the case for materials in which domain wall motion normally occurs more easily.

The application of a positive electric bias field parallel to the polar axis of a piezoelectric ceramic specimen is expected to cause a reduction in the high field dielectric and piezoelectric coefficients, due to a reduced domain wall mobility, in a similar manner to the effects described above for a static compressive stress. In contrast, a negative electric field applied in the direction antiparallel to the polar direction should cause a destabilising effect, thereby increasing the high field dielectric and piezoelectric coefficients. Schaufele and Hardtl have already confirmed that an electric bias can be employed to modify the mechanical depolarisation behaviour of PZT ceramics, as noted above, with a positive bias acting to increase the coercive stress X_c [36].

The stabilising effect of a positive DC bias field has been confirmed in our own work on soft PZT ceramics, as shown in Fig. 29 [48]. Here, it is apparent that the dielectric loss in soft PZT ceramics, measured at high fields, can be reduced remarkably by the application of a bias field. However, the remaining dielectric loss under bias is still too high for such materials to be considered for high power applications. Furthermore, the piezoelectric coefficients are also likely to be reduced in the presence of a positive bias field.

Perrin *et al.* have recently shown that the application of a negative bias field causes an increase in ϵ_{33} and d_{33} for both soft and hard PZT ceramics, as shown in Figs 30 and 31 [49]. The effect of a positive bias field for the hard PZT was less straightforward in that the dielectric permittivity ϵ_{33} was found to reduce slightly while d_{33} increased a little (Fig. 31). It is likely that the expected reduction in these coefficients due to the change in domain wall mobility caused by the bias field is obscured by the deaging effects, which are also induced by the bias field. This behaviour reflects the observations made above concerning the influence of static stress on the dielectric and piezoelectric properties, suggesting that

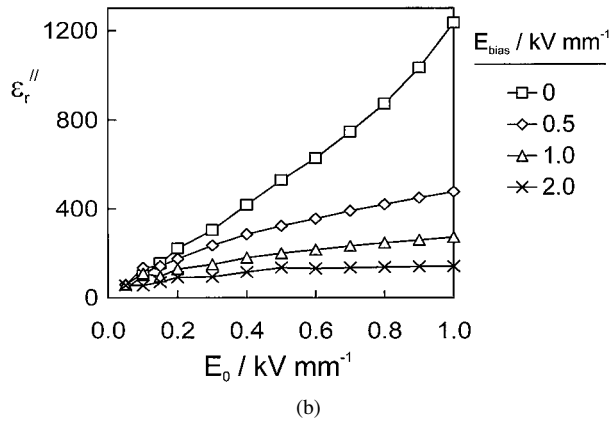
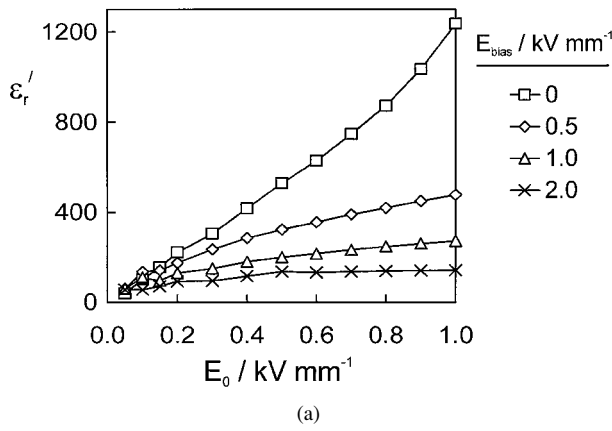


Figure 29 Variation of dielectric properties of PZ27 soft PZT ceramic as a function of field amplitude at 30 °C, various bias fields (a) ϵ_r' - E_0 , (b) ϵ_r'' - E_0 , after Stevenson *et al.* [48].

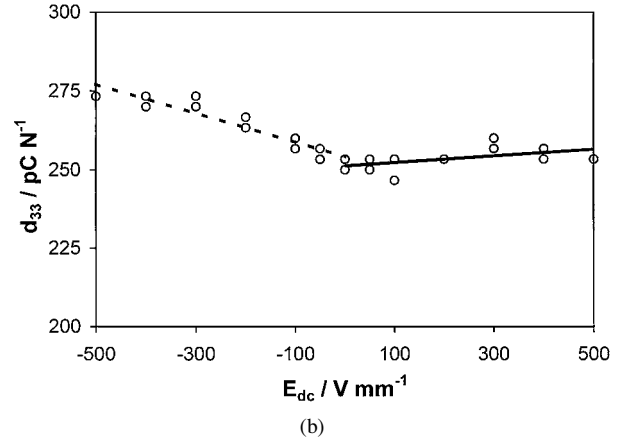
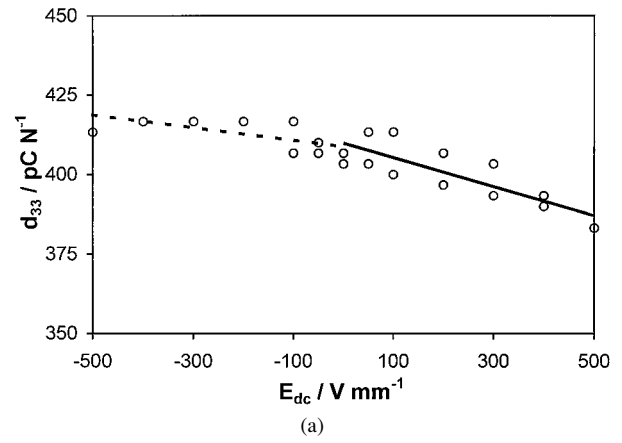


Figure 31 Piezoelectric strain coefficient d_{33} as a function of DC bias field for (a) soft PZT and (b) hard PZT ($f = 1$ kHz, $E_0 = 30$ V mm⁻¹), after Perrin *et al.* [49].

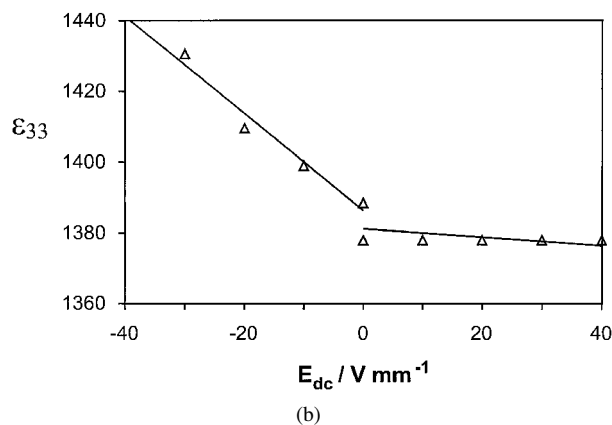
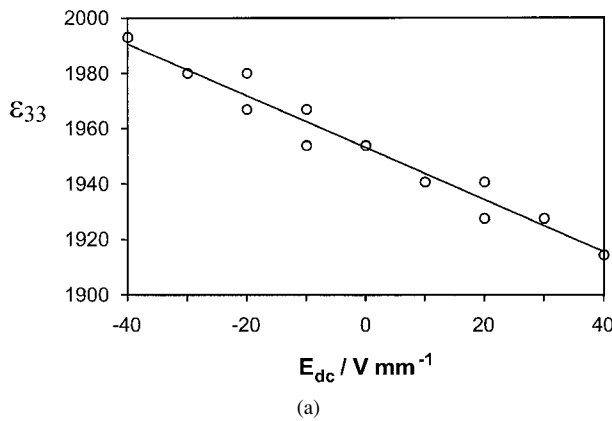


Figure 30 Dielectric permittivity ϵ_{33} as a function of DC bias field for (a) soft PZT and (b) hard PZT ($f = 1$ kHz, $E_0 = 3$ V mm⁻¹), after Perrin *et al.* [49].

both effects can be understood, at least qualitatively, in terms of the same underlying mechanisms.

3. Thermodynamic approach to nonlinear behaviour

3.1. Derivation of linear constitutive relations

Damjanovic recently provided a thorough review of the thermodynamic relations in piezoelectric ceramics [50]. This approach is summarised in the following sections, in order to highlight the inherent assumptions, and then extended to encompass nonlinear behaviour following the method proposed by Joshi [51].

The reversible change dU in internal energy U for an elastic dielectric subjected to a small change of strain dx_{ij} and electric displacement dD_i is, under isothermal conditions:

$$dU = X_{ij}dx_{ij} + E_i dD_i \quad (39)$$

The Gibbs free energy of a piezoelectric material under isothermal conditions can be written as:

$$G = U - X_{ij}x_{ij} - E_i D_i \quad (40)$$

The resulting change dG in G is given by:

$$dG = dU - X_{ij}dx_{ij} - x_{ij}dX_{ij} - E_i dD_i - D_i dE_i \quad (41)$$

Substituting Equation 39 into 41 yields:

$$dG = -X_{ij}dx_{ij} - D_i dE_i \rightarrow dG = -X_{ij}dx_{ij} - D_i dE_i \quad (42)$$

It follows that:

$$x_{ij} = -\left(\frac{\partial G}{\partial X_{ij}}\right)_E \quad \text{and} \quad D_i = -\left(\frac{\partial G}{\partial E_i}\right)_X \quad (43)$$

In general, for a function f of two independent variables, say $f(x, y)$, then the total differential df of f can be expressed as a Taylor series involving the partial differentials of f with respect to x and y :

$$\frac{\partial^3 f}{\partial x^3} dx^3 \rightarrow \frac{\partial^3 f}{\partial x^3} dx^3$$

and

$$\frac{\partial^3 y}{\partial y^3} dy^3 \rightarrow \frac{\partial^3 f}{\partial y^3} dy^3 \quad (44)$$

In the conventional approach, the Taylor expansions for strain x and dielectric displacement D are limited to the first order terms, giving:

$$dx_{ij} = \left(\frac{\partial x_{ij}}{\partial X_{kl}}\right)_E dX_{kl} + \left(\frac{\partial x_{ij}}{\partial E_k}\right)_X dE_k \quad (45)$$

$$\text{and} \quad dD_i = \left(\frac{\partial D_i}{\partial X_{jk}}\right)_E dX_{jk} + \left(\frac{\partial D_i}{\partial E_j}\right)_X dE_j \quad (46)$$

It is assumed that the partial derivatives can be represented by the following constants:

$$S_{ijkl}^E = \left(\frac{\partial x_{ij}}{\partial X_{kl}}\right)_E \rightarrow s_{ijkl}^E = \left(\frac{\partial x_{ij}}{\partial X_{kl}}\right)_E \quad (47)$$

$$d_{kij}^X = \left(\frac{\partial x_{ij}}{\partial E_k}\right)_X = \left(\frac{\partial D_k}{\partial X_{ij}}\right)_E = d_{kij}^E$$

= piezoelectric charge/strain coefficient

$$(48)$$

$$\varepsilon_{ij}^X = \left(\frac{\partial D_i}{\partial E_j}\right)_X$$

= absolute dielectric permittivity

$$(49)$$

It is usual to take the reference levels of strain and dielectric displacement as zero and then use the reduced, or matrix notation which makes use of the symmetry of the stress and strain tensors. Then, the constitutive equations can be written in the simplified form given earlier:

$$x_m = S_{mn}^E X_n + d_{im}^X E_i \quad (1)$$

$$D_i = d_{im}^E X_m + \varepsilon_{ij}^X E_j \quad (2)$$

with $i, j = 1..3$ and $m, n = 1..6$.

It should be noted that for Equation 1 the $[d]$ matrix should be transposed to $[d]^T$ in order to conform to standard matrix algebra. Then, we can write:

$$[x] = [s^E][X] + [d]^T [E] \quad (50)$$

$$x_m = S_{mn}^E X_n + d_{im}^X E_i \rightarrow x_m = s_{mn}^E X_n + d_{im}^X E_i \quad (51)$$

Alternative forms of the constitutive equations can be derived using other thermodynamic potentials, chosen with regard to different combinations of independent and dependent variables (from E, D, x, X) [50].

3.2. Derivation of nonlinear constitutive relations

First order nonlinearity in the dielectric, elastic and piezoelectric properties of piezoelectric ceramics can be obtained by extending the Taylor series expansion to include the second order partial derivatives, using the form of Equation 44. This yields the following expressions for the total differentials of strain and dielectric displacement:

$$dx_{ij} = \left(\frac{\partial x_{ij}}{\partial X_{kl}}\right)_E dX_{kl} + \left(\frac{\partial x_{ij}}{\partial E_k}\right)_X dE_k$$

$$+ \frac{1}{2} \left[\left(\frac{\partial^2 x_{ij}}{\partial X_{kl} \partial X_{mn}}\right)_E dX_{kl} dX_{mn} + 2 \left(\frac{\partial^2 x_{ij}}{\partial X_{kl} \partial E_m}\right) \times dX_{kl} dE_m + \left(\frac{\partial^2 x_{ij}}{\partial E_k \partial E_l}\right)_X dE_k dE_l \right] \quad (52)$$

$$\frac{\partial^2 D_i}{\partial X_{ik} \partial X_{lm}} \rightarrow \frac{\partial^2 D_i}{\partial X_{jk} \partial X_{lm}} \quad (53)$$

By setting the reference values of field-induced dielectric displacement and strain to zero and using the reduced matrix notation, Equations 52 and 53 can be written in a simpler form as:

$$k_{imn} X_n E_i \rightarrow \kappa_{imn} X_n E_i \quad (54)$$

$$k_{imn} X_n E_i \rightarrow \kappa_{imn} X_n E_i \quad (55)$$

where the nonlinear dielectric, elastic and piezoelectric coefficients are given by:

$$s_{mnp}^E = \left(\frac{\partial^2 x_m}{\partial X_n \partial X_p}\right)_E$$

$$d_{ijm} = \left(\frac{\partial^2 x_m}{\partial E_i \partial E_j}\right)_X = \left(\frac{\partial^2 D_i}{\partial X_m \partial E_j}\right)$$

$$\varepsilon_{ijk}^X = \left(\frac{\partial^2 D_i}{\partial E_j \partial E_k}\right)_X$$

$$\kappa_{imn} = \left(\frac{\partial^2 x_m}{\partial X_n \partial E_i}\right) = \left(\frac{\partial^2 D_i}{\partial X_m \partial X_n}\right)_E \quad (56)$$

It is evident from Equation 54 that s_{mnp}^E and d_{ijm} represent first order nonlinearity in the elastic compliance and piezoelectric strain coefficient respectively. Also, from Equation 55 ε_{ijk}^X and κ_{imn} represent first order nonlinearity in the dielectric permittivity and the piezoelectric charge coefficient respectively. Note that d_{ijm} and κ_{imn} , representing the nonlinear components of the converse and direct piezoelectric effects respectively, are not equivalent.

It is apparent that d_{ijm} may also be used to represent the cross-coupling between the nonlinear components of dielectric displacement induced by simultaneously applied electric field E and mechanical stress X in Equation 55. Similarly, κ_{imn} represents cross-coupling between the nonlinear components of strain in Equation 54. Potentially, this provides a useful means of determining these cross-coupling coefficients from a series of measurements under zero stress (for d_{ijm}) or zero electric field (for κ_{imn}), thereby avoiding the need

for lengthy studies in which both E and X must be controlled simultaneously. It remains to be seen whether these relationships can be validated in practise.

As noted above (Section 2.5), superficially these relationships appear to have the same form as the Rayleigh Law, but in fact do not accurately predict the magnitudes of the harmonic components of x and D for a cyclic stress or electric field waveform.

4. Hysteretic models of nonlinearity

4.1. Hysteresis due to domain wall motion

The traditional approach to modelling hysteretic behaviour of materials (ferromagnetic, ferroelastic and ferroelectric) is a phenomenological one, in that mathematical models are sought to describe a range of experimental observations. Ultimately, physical models can be developed in order to relate key parameters in the model to physical quantities such as the domain wall density and mobility, dislocation density etc. Studies of the Rayleigh Law in ferromagnetic materials provide a useful illustration of this approach.

Lord Rayleigh first reported in 1887 that the magnetic permeability of iron and steel increased linearly with field amplitude, over a range of field strengths below the coercive field, as described above [20]. Furthermore, the B-H (magnetic induction-magnetic field) relationship could be approximated by a combination of 2 parabolic functions, corresponding to the ascending and descending branches of the minor hysteresis loop. These are the first and second Rayleigh relations, which can be expressed as:

$$\mu(H_0) = \mu(0) + \alpha H_0 \quad (57)$$

$$B(H) = (\mu(0) + \alpha H_0)H \pm \frac{\alpha}{2}(H_0^2 - H^2) \quad (58)$$

The resulting idealised hysteresis loop, given in terms of the associated magnetisation-field relationship is illustrated in Fig. 32.

This form of hysteretic behaviour was interpreted by Weiss and Freudenberg [53], and then by Preisach [54], in terms of an assembly of magnetic regions, within which the magnetisation could be reversed either reversibly or irreversibly. Subsequently, Neel suggested that a more realistic interpretation for a soft ferromagnetic or ferrimagnetic material would treat

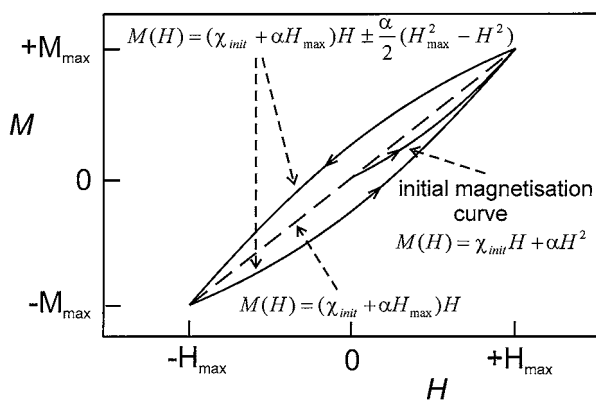


Figure 32 Idealised M-H loop illustrating Rayleigh relations, after Damjanovic [52].

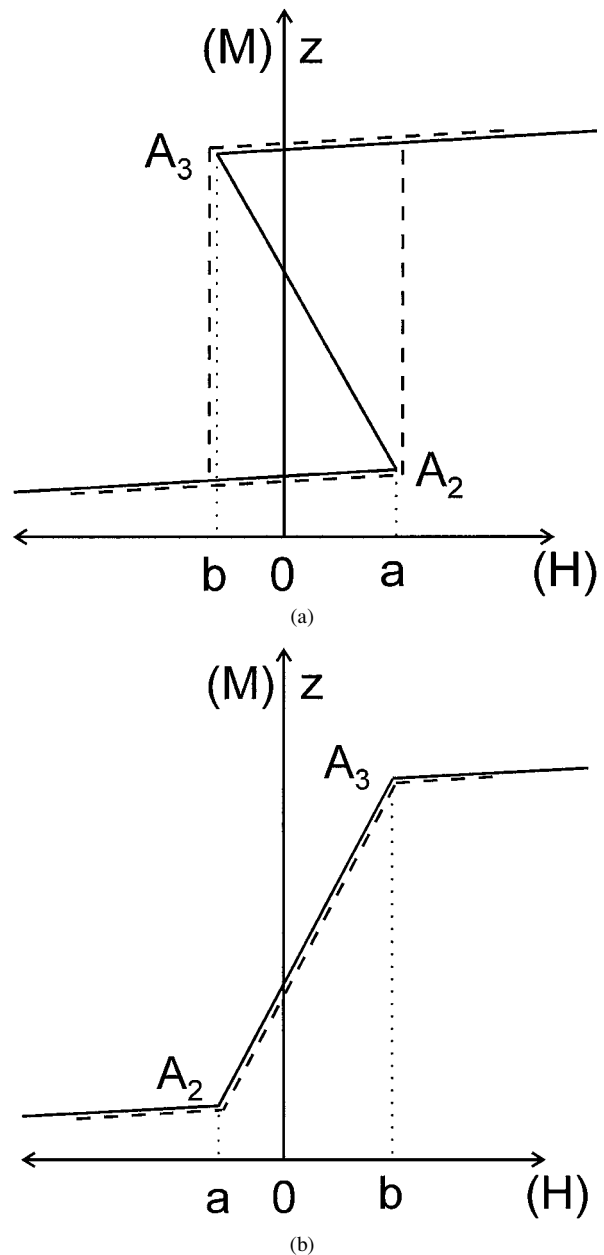


Figure 33 (a) Irreversible and (b) reversible imaginary cycles corresponding to small wall displacements against an opposition represented by straight lines, after Neel [56].

these irreversible and reversible magnetisation cycles as imaginary cycles corresponding to successive partial displacements of domain walls, as shown in Fig. 33 [55, 56].

Magnetisation cycles of this type can be categorised according to the relative values of the critical switching fields a and b , those with $a < b$ representing reversible cycles and those with $a > b$ irreversible cycles. By assuming a certain statistical distribution of a and b pairs (actually a uniform distribution of points around the origin in the a - b plane), it is possible to calculate both the reversible and irreversible components of magnetisation for any given path of the applied field, and hence to derive the two Rayleigh relations [56]. A similar approach is used in Preisach-type models, where the switching events are used to represent the reversal of magnetisation within collections of bi-stable units [57].

The model developed by Neel served as the basis for subsequent studies in which closer links were sought

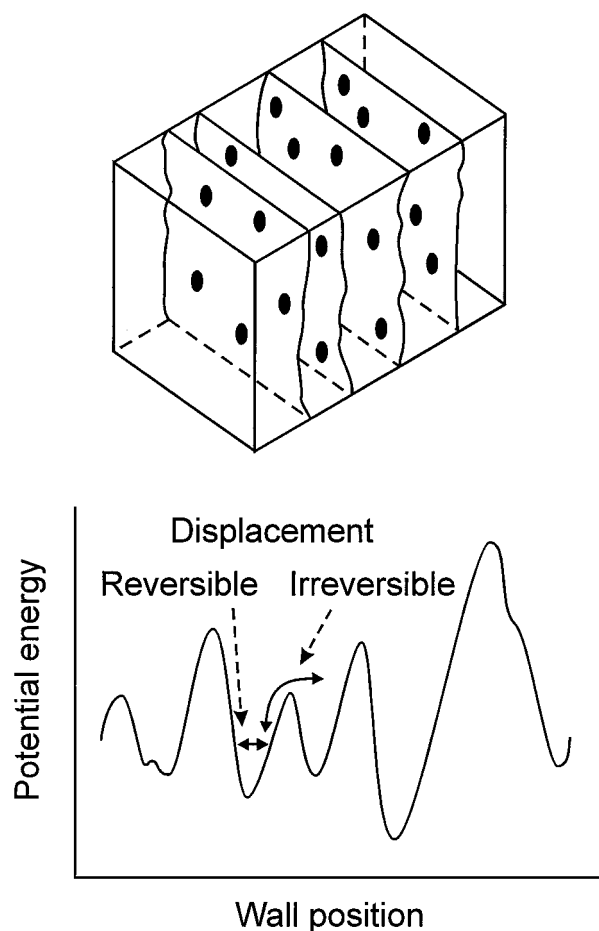


Figure 34 Schematic illustration of interaction of domain walls with randomly distributed pinning centres (above) and the corresponding energy profile associated with the domain wall position (below), after Damjanovic [62].

between the mathematical form of the model and measurable physical parameters [58]. Microstructural features (such as grain size) and dislocation density have been shown to influence factors such as the initial permeability, Rayleigh coefficient and coercive field. The results of such studies are usually interpreted in terms of the changes in the random periodic domain wall potential caused by the presence of microstructural or crystal defects [59–61].

It is evident from the results presented above that the nonlinear dielectric and piezoelectric properties of ferroelectric ceramics are represented well by the Rayleigh relations. The range of electric field strength or stress over which the Rayleigh behaviour occurs corresponds closely to those experienced in service by piezoelectric actuator materials. The mechanism responsible for Rayleigh behaviour in ferroelectrics is illustrated in Fig. 34 [62]. Here, it is supposed that the domain wall potential can be represented by a periodic function with a random distribution of barrier heights, due to its interaction with an array of pinning defects. The domain wall can move reversibly over small distances within the first potential well surrounding its equilibrium position. This type of nonhysteretic domain wall vibration provides a contribution to the dielectric, elastic and piezoelectric properties even at low field strengths, as described above (Section 2.1).

A certain ‘threshold field’ E_t is required to initiate large scale domain wall translation across the array of pinning defects, giving rise to the hysteretic response. The dielectric, elastic and piezoelectric phenomena associated with the domain wall translation mechanism can also be understood in terms of the combination of reversible and irreversible imaginary cycles described by Neel.

Boser adapted this approach to describe the dielectric properties of ferroelectrics and showed how certain measurable parameters such as the initial permittivity, Rayleigh coefficient and coercive field could be related to the form of the domain wall potential, or force profile [63]. The origin of the force profile itself was also derived on the basis of the interaction energies between point defects and the domain wall. Although only limited experimental data were available, it did appear that the Rayleigh coefficient α was inversely proportional to the defect concentration in Fe-doped barium titanate ceramic, as was predicted by the model.

Damjanovic [52] and Kugel [31] have both shown how the Rayleigh relations can be used to model the strain-field and dielectric displacement-field relationships in ferroelectric ceramics. Furthermore, the growth of higher frequency harmonic signals can also be predicted from hysteretic models of this type [20, 31, 52]. It should be noted that the observed nonlinearity in piezoelectric ceramics does not always follow the ideal Rayleigh model. However, the Rayleigh relations can be viewed as one possible consequence of a more general hysteretic model which can include higher order terms, as discussed by Damjanovic [52] and Kugel [31]. Therefore, deviations from the Rayleigh Law could be accommodated by introducing a greater level of complexity into the underlying hysteretic relationship. In physical terms, this could be viewed as indicating differences in the domain wall force profile, perhaps caused by the asymmetry associated with the preferred polarisation direction in a poled ferroelectric specimen or ‘clamping’ of the domain walls by dipolar defect associates.

Damjanovic *et al.* have argued that the Preisach model can serve as a very useful tool for interpreting nonlinearity and hysteresis in the dielectric and piezoelectric properties of ferroelectric ceramics [64]. In their description, which was based on the approach of Bertotti [57], the hysteretic response of a property R (e.g. strain, polarisation) is described in terms of the internal field F_i and the coercive field F_c of a bi-stable unit, as shown in Fig. 35. The macroscopic response of an assembly of such bi-stable units is governed by a function $f(F_i, F_c)$, which defines the distribution of bi-stable units over the F_i - F_c plane. As with the approach of Neel [55, 56], a constant distribution function gives rise to the Rayleigh Law. On the other hand, deviations from the Rayleigh Law can be readily interpreted in terms of a slightly uneven distribution function f . For example, the existence of a finite threshold field for nonlinearity, F_t , indicates that there are few bi-stable units present having low values of F_i and F_c , less than F_t . In this case, a finite value of the applied field, greater than F_t , must be reached before the assembly of

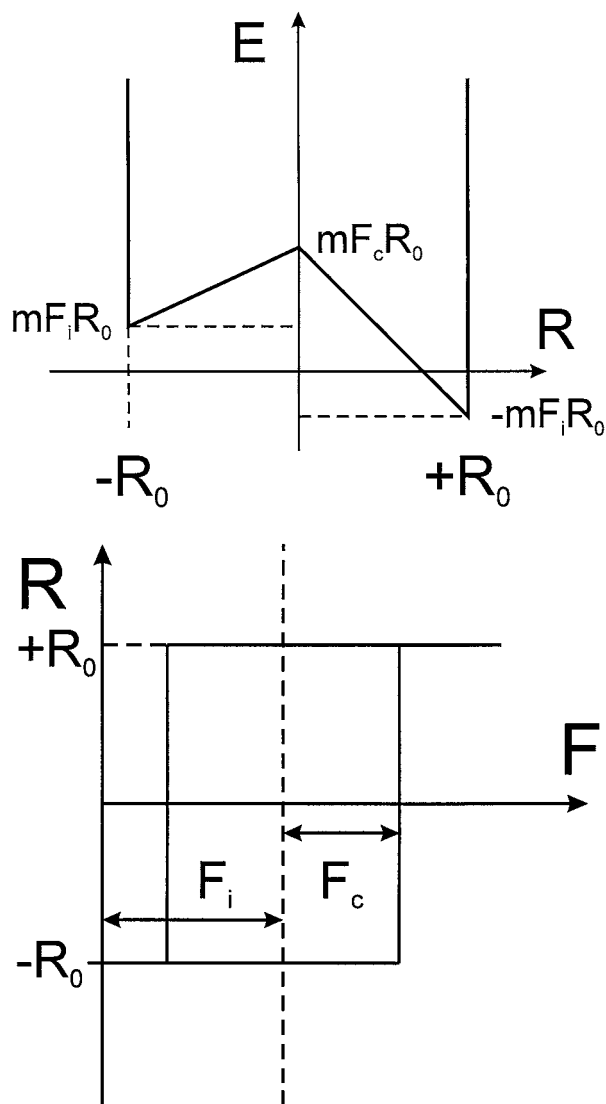


Figure 35 The energy (E) and hysteresis of an elementary bi-stable unit (m is a generalized susceptibility), after Damjanovic *et al.* [64].

bi-stable units can begin to contribute to the macroscopic response R .

The Rayleigh Law in ferroelectrics could conceivably be interpreted in terms of a hysteretic polarisation mechanism completely separate to that of domain wall translation. This could occur if the domain walls were so strongly pinned that reverse domain nucleation occurred before significant movement of existing walls. The polarisation switching mechanisms described below represent one possible explanation of nonlinear behaviour, since partial domain switching at field levels below the macroscopic coercive field could give rise to dielectric and piezoelectric coefficients that increase as a function of the electric field level.

The main practical difficulty in implementing a phenomenological model of nonlinearity in piezoelectric ceramics is likely to be the problem of characterising all of the relevant nonlinear coefficients. This task may be fairly straightforward in a monolithic ceramic component, where the electric field and stress might be considered as uniform to a first approximation and only a limited number of tensor coefficients need to be considered. However, it could be an insurmountable problem

when the stress and electric field distributions within a multilayer device are required, in which case the full dielectric, elastic and piezoelectric tensors are required. For this reason, it would be very desirable to have access to a micro-mechanical model, within which the required nonlinear tensor components could be calculated from a smaller number of measurable values.

4.2. Hysteresis due to polarisation switching

To date, most of the publications on micro-mechanical modelling have employed a domain switching argument. With this approach, it is usually proposed that a piezoelectric ceramic is made up from an array of single domain grains and that ferroelectric or ferroelastic switching can occur when the energy provided by the applied electric or stress field exceeds a critical value. This so-called 'energy criterion' method is expressed in the following relation [65]:

$$E_i \Delta P_i + X_{jk} \Delta x_{jk} \geq 2 P_s E_{crit} \quad (59)$$

where P_s is the spontaneous polarisation and E_{crit} is the critical field for polarisation switching.

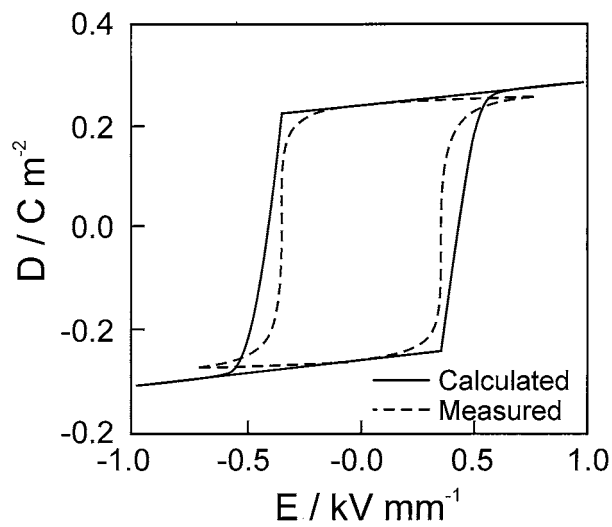
The P - E and x - E relationships predicted from such models can usually simulate the main features of the experimental data obtained at saturation (Fig. 36), but the simplifying assumptions (e.g. no ferroelectric domains within a grain) cast some doubt on the physical validity of the model.

Increasing sophistication of such models has enabled the effect of a static stress to be considered, as shown in Fig. 37. In this case, the influence of grain to grain interaction (i.e. the effect of 1 grain switching on the behaviour of the surrounding grains) was incorporated into the model using a mean field method [66].

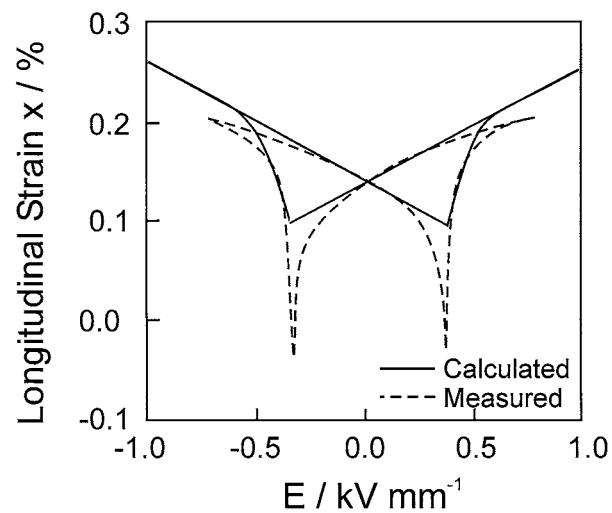
As an alternative approach, a finite element method was also investigated by Hwang and McMeeking, based on a similar switching criterion [67]. The grain to grain interactions of a polycrystalline ferroelastic solid were modelled using a $10 \times 10 \times 10$ cubic array of grains. Hysteretic stress-strain relationships were simulated using a range of different values for the switching energy. This model illustrated the manner in which one crystallite inhibits the switching of a neighbouring one, with the result that a significant coercive stress is required to initiate the switching process, even when the critical switching stress for each individual crystallite is very low.

It was noted by Hwang and McMeeking that the micro-mechanical models developed did not provide a very close correspondence to experimental data, and that the computational effort required to produce the simulation would make it unsuitable for incorporation in a complex 3-dimensional problem. Rather, the value of such models lies in the insight that they can provide into the mechanisms responsible for nonlinear behaviour and as a guide for the development of macroscopic constitutive laws [67].

One of the limitations of the micro-mechanical models developed by Hwang *et al.* lies in their neglect of ferroelectric domain formation, and of the details of the polarisation switching mechanism. As a result, it



(a)



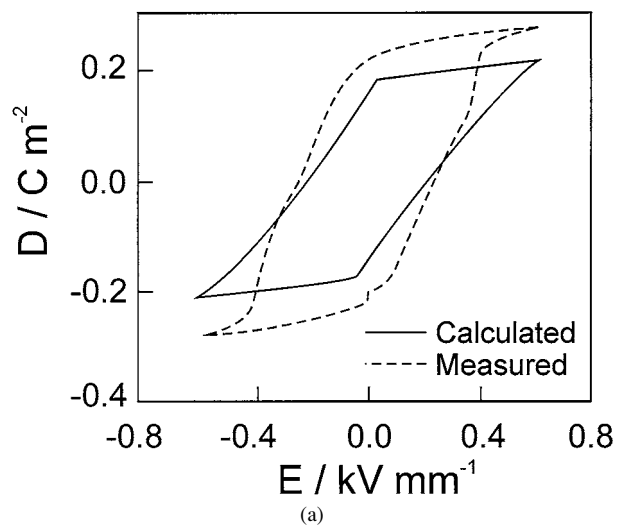
(b)

Figure 36 Comparison of simulated and measured (a) D - E and (b) x - E hysteresis loops for 8/65/35 PLZT using the energy criterion for polarisation switching, after Hwang *et al.* [65].

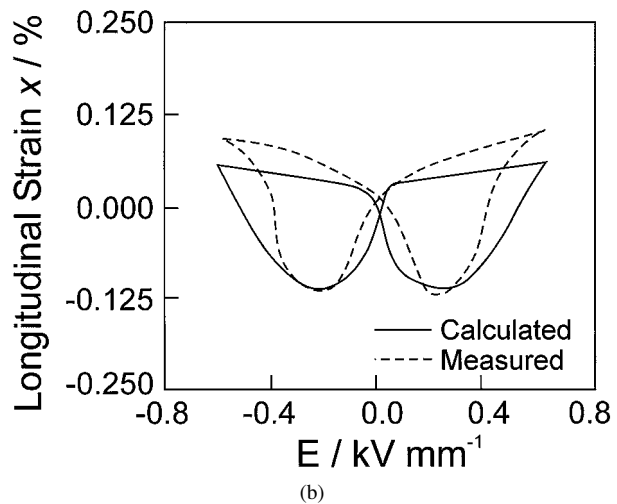
is debatable whether the fitting parameters used in the models can accurately represent the physical properties of the materials in question. It is well known that ferroelectric domain formation occurs on cooling through the Curie temperature T_c , in order to minimise the electrostatic and elastic energies [68–72]. The elastic energy term is usually considered to be the most significant, since the electrostatic field associated with a polar domain can be neutralised, over a time period equal to the dielectric time constant, $\tau = \rho\epsilon$, by the migration of free charges.

Arlt *et al.* have developed models to describe the state of residual stress associated with simple laminar 90° domain stacks and with more complex herringbone-type domain configurations, as illustrated in Fig. 38 [69–72]. It can be noted that the average spontaneous strain x_g and polarisation P_g of a grain containing such a domain pattern will be significantly reduced relative to the single domain values x_0 and P_0 . The magnitude of the residual stress in a polycrystalline ceramic is thereby reduced considerably by domain formation.

The mechanisms for polarisation reversal in ferroelectric ceramics have remained elusive, in contrast to the case in single crystal ferroelectrics where the do-



(a)



(b)

Figure 37 Comparison of simulated and measured (a) D - E and (b) x - E hysteresis loops for 8/65/35 PLZT with a static compressive stress of 15 MPa, after Hwang *et al.* [66].

main switching process can be observed directly by optical microscopy techniques [43]. Visual observations using either optical or electron microscopy, are hampered by the very fine scale of the domain patterns (domain widths are often less than $0.1 \mu\text{m}$) and the lack of elastic constraint in the thin or polished sections which are necessary for such investigations. Modern force microscopy techniques offer one possible solution to this problem, although even with these methods it is not easy to observe the domain switching processes dynamically.

Arlt proposed a ferroelectric domain switching mechanism based on the nucleation of a new transient domain wall within an existing laminar 90° stack, as shown in Fig. 39a [73, 74]. A certain energy barrier must be overcome to create this wall, in order to accommodate the associated elastic energy (Fig. 39b). Once nucleated, this transient domain wall can sweep through the grain without hindrance, thereby switching its polarisation through 180° . This type of domain reversal process does not involve any net change in elastic energy, since the overall shape of the grain is the same before and after switching.

On this basis, Arlt proposed an alternative model of domain switching based purely on electrostatic considerations [74, 75]. It was shown that the P - E hysteresis

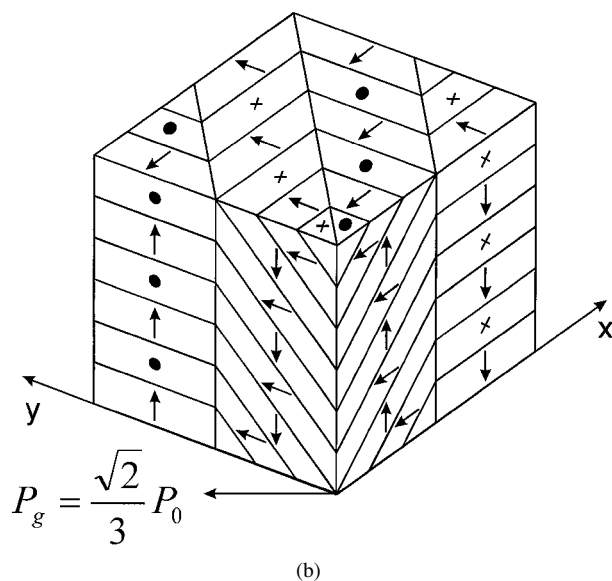
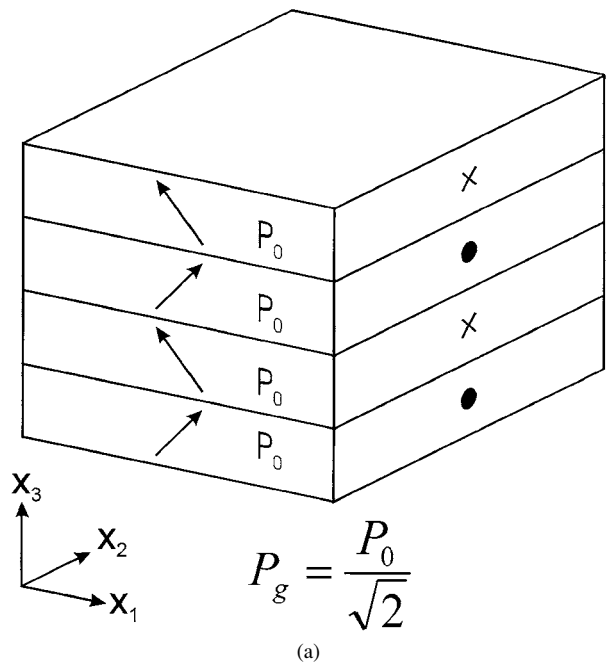


Figure 38 Domain configurations of tetragonal ferroelectric ceramics. The laminar stack on the left is representative of fine-grained materials while the banded 'herringbone' structure on the right represents coarse-grained materials, after Arlt [73].

curves for both barium titanate and PLZT ceramics could be simulated with this model, using reasonable values for the grain polarisation, critical switching field, and dielectric permittivity of the materials. It was also suggested that the nonlinear properties of ferroelectric ceramics could be interpreted in a similar manner, as being due to partial domain switching at field levels below the macroscopic coercive field.

The micro-mechanical polarisation switching approach has been taken a step further by Steinkopff, who described the incorporation of such a model into a 3D piezoelectric element in the finite element program ANSYS [76]. Although the full details of the methods used to implement the model were not described, it was demonstrated by Schuh *et al.* that the nonlinear elastic and piezoelectric behaviour at sub-switching fields give rise to an effective 'softening' of the ceramic within regions in piezoceramic components experiencing high

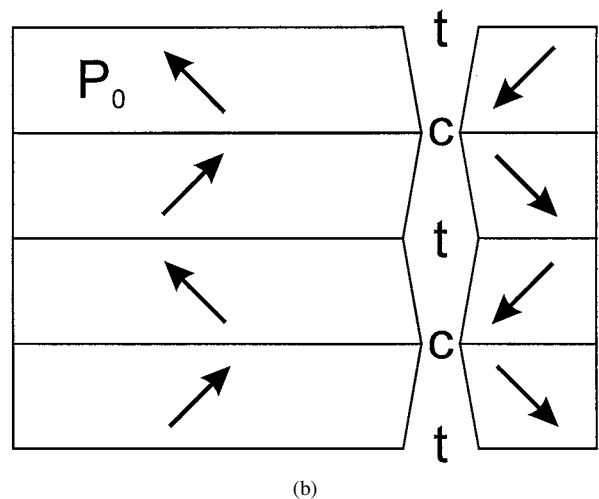
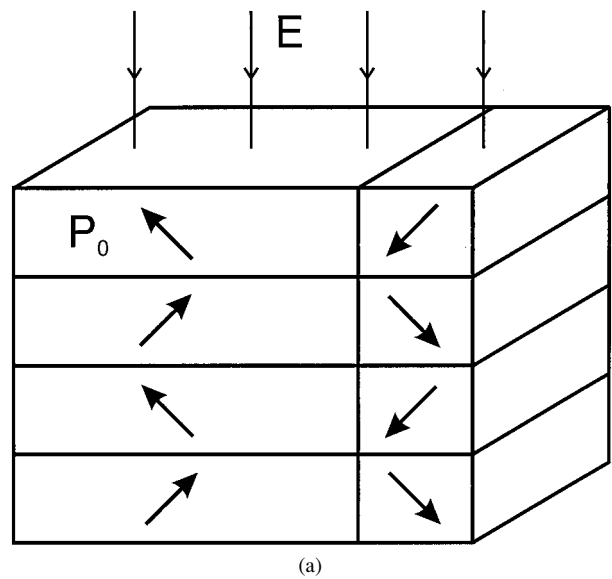


Figure 39 Schematic diagram illustrating (a) the generation of a new transient domain wall within a 90° domain stack, which is generated at the grain boundary and traverses the grain from left to right without deforming it (b) deformations associated with the transient domain wall which have to be smoothed by elastic stresses, after Arlt [75].

levels of strain [77]. This effect had the important practical consequence that the levels of stress in the 'inactive' regions of a multilayer piezoelectric actuator, around the electrode edges, were considerably lower than that which would be predicted by a linear analysis.

The LGD (Landau-Ginzburg-Devonshire) thermodynamic theory of ferroelectric phase transformations can also be used to model the nonlinear behaviour of ferroelectrics. This method is based on expressing the Gibbs free energy as a function of the appropriate order parameter (typically polarisation or dielectric displacement). The method can be used to describe the main characteristics of the paraelectric-ferroelectric phase transformation [43], and has been extended recently to form a basis for understanding the switching characteristics of ferroelectrics [78]. For example, the ferroelectric P - E hysteresis loop can be derived from an equation of the form:

$$G = \frac{\alpha}{2}D^2 + \frac{\gamma}{4}D^4 + \frac{\delta}{6}D^6 \quad \text{where } \alpha = \beta(T - T_c) \quad (60)$$

which leads to:

$$E = \left(\frac{\partial G}{\partial D} \right)_T = \alpha D + \gamma D^3 + \delta D^5 \quad (61)$$

One limitation of this method is that in its usual form it does not account for the presence of lattice defects, grain boundaries, or ferroelectric domains. As a result of this, the absolute value of the coercive field derived from such a model can be several orders of magnitude larger than that found experimentally in ferroelectric ceramics [43].

Van Rensburg and Humberstone adopted this approach as part of NPL project AM4 [79]. The aim of this work was to provide a simple model for ferroelectric hysteresis, employing relatively few parameters, that could be used as a predictive tool for modelling the performance of piezoelectric ceramic devices. Their method was based on a simple 1-dimensional model of a 180° domain wall in an isolated ferroelectric crystal. The change in polarisation resulting from an applied electric field was achieved by movement of the domain wall, assuming the following rate equation:

$$v_w = v_0 e^{-\frac{\delta}{E}} \quad (62)$$

where v_w is the wall velocity, v_0 is a constant, and δ is a coefficient describing the electric field ‘sensitivity’ of the wall motion. An additional rate constant γ_R was also introduced to describe the effect of an unspecified relaxation process, which was thought to be possibly thermal in origin. All other parameters in the model were derived from standard data tables for piezoelectric ceramics. In this manner, it was possible to simulate the main features of the saturated P - E and x - E hysteresis loops in soft ferroelectric ceramics.

The authors did not explore the feasibility of using the model to simulate nonlinearity in the sub-switching region, since it was designed primarily with regard to the saturated hysteresis loops. Also, it is questionable whether an expression of the form given in equation 62 could properly describe domain wall movement in a ferroelectric ceramic at field levels below the macroscopic coercive field, since it predicts a finite domain wall velocity even at relatively low fields. Given sufficient time under a DC field, or a low frequency alternating sinusoidal signal, even a relatively slow domain wall movement could cause complete polarisation reversal, giving rise to saturated P - E and x - E relationships. This clearly does not follow experimental observations in most piezoelectric ceramics, since the majority of domain walls will move only a limited distance if $E < E_c$. Therefore, without further development this model is unlikely to provide an accurate description of nonlinearity at sub-switching field levels.

4.3. Path-dependent hysteresis

Hysteretic phenomena are particularly problematic in micropositioning applications, with the result that closed-loop control systems incorporating displacement sensors must be used when a high positioning accuracy is required. One approach described by

Newcomb and Flynn [80] is to control the electric charge rather than voltage, which yields much improved linearity, as would be expected from the near-linear strain-dielectric displacement (charge density) relationship described by Kugel and Cross [31]. However, this method would require the use of a specially designed charge drive amplifier which increases the hardware costs significantly.

Ge and Jouaneh have shown how a Preisach-type model can be used to more accurately predict the hysteretic and path-dependent field-displacement relationship of a piezoelectric actuator [81, 82]. Certain modifications to the classical Preisach model were required to take account of the unipolar drive which is commonly used for piezoelectric actuators and the presence of a mechanical bias, which was considered to be the origin of asymmetry in the displacement-voltage relationship [81].

The development of a numerical Preisach model, which could be used to predict the response of a given piezoceramic actuator, involved the determination of a series of first order reversal curves within a ‘major’ hysteresis loop, as illustrated in Fig. 40. The data collection routines required by this approach were automated, such that the major loop at a given maximum drive voltage and 10 first order reversal curves could be collected within 10 s. Intermediate values required for the model were then obtained by interpolation between values derived from these first order reversal curves. It was shown that the model enabled the displacement characteristics of a piezoelectric actuator in response to a continuous sinusoidal voltage signal to be simulated with an accuracy of 3% [81].

In a subsequent paper [82], the same authors showed how the sophistication of the model could be improved by incorporating a series of second order reversal curves (Fig. 40). With suitable modifications, it was possible to simulate the displacement response from an actuator due to an arbitrary input signal to within 3%, as shown

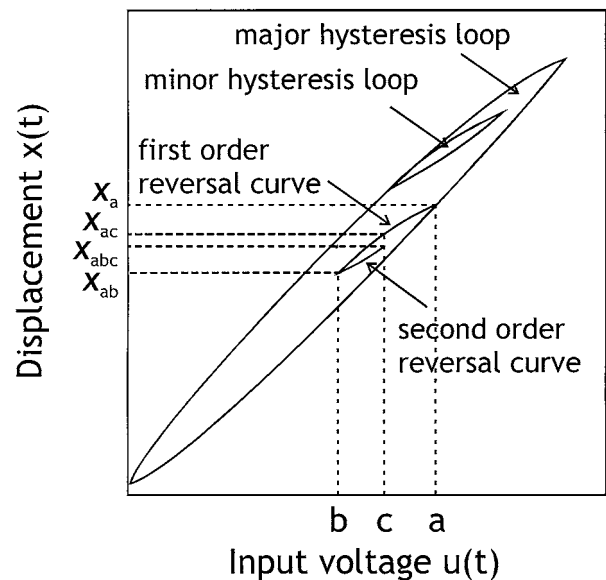


Figure 40 Illustration of the displacement-voltage characteristic of a piezoceramic actuator, showing a first-order and a second-order reversal curve, and a major and a minor hysteresis loop, after Ge and Jouaneh [81].

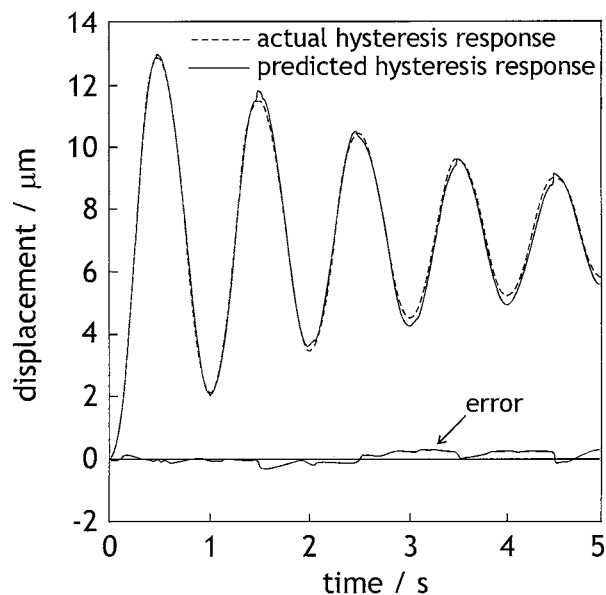


Figure 41 Comparison of actual and predicted hysteresis response of a piezoceramic actuator under an exponentially decaying sinusoidal excitation, after Ge and Jouaneh [82].

in Fig. 41. The model was subsequently incorporated into the control system for a piezoelectric positioning device and was found to give a significant improvement in positioning accuracy.

5. Summary and comparison of models for nonlinearity in piezoelectric ceramics

A large body of experimental data has been published concerning the nonlinear properties of piezoceramics, as described in Section 2 above. It is clear that in most ferroelectric ceramics the dielectric, elastic and piezoelectric coefficients increase considerably with field/stress amplitude, even at sub-switching levels. In many cases, it has been shown that the relevant coefficients increase in an almost linear fashion with field/stress amplitude, according to the Rayleigh Law. This provides a fairly straightforward means of modelling the nonlinear dielectric and piezoelectric properties of piezoceramic components, provided that the relevant nonlinear dielectric and piezoelectric coefficients can be measured and that the electric field and stress can be considered as uniform within the component. The generation of higher frequency harmonic components through the nonlinear dielectric or piezoelectric coefficients can also be interpreted in terms of a Rayleigh-type hysteretic relationship, which could be useful in modelling the performance of high power piezoelectric transducers.

The value of the threshold field/stress for nonlinear behaviour, as well as the frequency and temperature-dependence of the nonlinear coefficients should all be available for accurate modelling of nonlinear behaviour in a wide range of operating conditions. The influence of a static electric field or stress should also be considered, since piezoelectric devices will often experience such conditions in practical operation. There are already indications that such effects can be mod-

elled in a fairly simple manner, although possible time-dependent deaging effects caused by partial domain switching under the influence of a static electric field or stress should not be ignored.

Simulation of the electric field and stress distributions within complex piezoceramic components (e.g. multilayer actuators) requires a knowledge of the nonlinear behaviour of the materials under the combined action of an alternating electric field and stress. This represents a very challenging problem, since to date the interactions between the nonlinear dielectric, elastic and piezoelectric tensor components have not been studied to any great extent. The thermodynamic theory (Section 3) suggests one approach, in which the nonlinear direct and converse piezoelectric coefficients could first be determined separately, under conditions of zero stress and zero electric field respectively, according to Equations 54 and 55. The validity of these coefficients as the cross-coupling terms could then be established by controlled experiments combining electric and mechanical loads. The nonlinear dielectric and elastic coefficients can be determined more easily by dielectric measurements under zero stress and stress-strain measurements under zero electric field respectively.

The development of a micro-mechanical model, based on either ferroelectric domain switching or domain wall translation is very attractive. Such a model could in principle provide the required tensor coefficients given a relatively small number of fitting parameters. Steinkopff [76] and Shuh [77] have already incorporated such a model, based on a polarisation switching mechanism, into a general purpose finite element code. The results presented by Shuh *et al.* [77] appear to show the expected reduction in stress within a multilayer actuator, due to 'softening' of the elastic modulus through the ferroelastic behaviour.

It is apparent from certain experimental observations that the dielectric and piezoelectric coefficients measured through the converse piezoelectric effect increase in an almost identical manner with increasing field amplitude (Figs 17, 18). This could provide a useful means of predicting the nonlinear piezoelectric coefficients from the more easily measured dielectric coefficients. Likewise, the direct proportionality between the real and imaginary coefficients that has been observed in the dielectric properties (Fig. 14) could provide a simple method for numerical modelling of the loss or phase angle as a function of field amplitude. Further experimental investigations could be devised to help establish the range of validity of these relationships.

None of the methods mentioned above would be appropriate for modelling the hysteretic and path-dependent effects that are observed in precision piezoceramic actuators. In this case, it has been shown by Ge and Jouaneh that a Preisach-type model can be applied to simulate the observed displacement-voltage relationships, eventually showing the ability to accurately predict the displacement resulting from an arbitrary input voltage signal [81, 82]. Conversely, such an approach would not be suitable for modelling the behaviour of a monolithic piezoceramic transducer operating under widely varying levels of stress and electric field or the

stress and electric field distribution within a complex piezoceramic component.

In terms of the physical models used to interpret the origin of nonlinear behaviour in ferroelectric ceramics at sub-switching levels of electric field and stress, the concept of domain wall translation is very convincing. This model seems able to explain the field and frequency-dependence of the dielectric, elastic and piezoelectric properties of piezoceramics within the Rayleigh range, which is of greatest importance for the practical operation of piezoelectric actuators and acoustic transducers. The dependence of characteristic nonlinear features such as the threshold field and Rayleigh coefficient on microstructure and composition (particularly the presence of acceptor-related point defects) can also be explained in quantitative fashion by such a domain wall translation model.

The concept of Rayleigh behaviour as one specific form of nonlinearity, represented in more general terms by a Preisach distribution function, provides further insight into the ferroelectric and ferroelastic switching events that are the origin of nonlinearity and hysteresis in piezoelectric ceramics [64]. It seems most likely that these switching events are associated with irreversible 'jumps' of ferroelectric domain walls as they traverse an array of pinning defects. This could provide the basis for an improved understanding of various phenomena in ferroelectrics, such as ageing and field/stress-induced deaging effects.

The polarisation switching mechanisms described above [65–67, 73–75] represent another possible explanation of nonlinear behaviour in the Rayleigh region, since partial domain switching at field levels below the macroscopic coercive field could give rise to a nonlinear and hysteretic contribution to the dielectric, elastic and piezoelectric properties that becomes more pronounced as the field level increases. However, the different types of nonlinear behaviour that are observed in ferroelectric ceramics below and above the coercive field seem to indicate that separate mechanisms are involved. It seems likely, therefore, that a domain wall translation mechanism is responsible for nonlinearity in the Rayleigh region below E_c , while domain switching is dominant above E_c . Distinguishing between these two mechanisms may not be straightforward, since both involve the reorientation of polarisation in a given small polar region. The use of a range of structural characterisation techniques (XRD, AFM, nano-indentation methods), in combination with field-induced polarisation and strain measurements, may be able to solve this problem.

An alternative hysteretic mechanism was suggested by Kugel and Cross [31], who proposed that the cooperative effects between ferroelastic grains (i.e. the field-induced inter-granular stresses) could be largely responsible for the hysteresis in ferroelectric ceramics. This point was also highlighted by Hwang and McMeeking [67], who predicted that a significant ferroelastic hysteresis could occur in a bulk ceramic material even when the individual grains had a very low critical switching stress. It should be recognised that the residual and field-induced inter-granular stresses in ferroelectric ceramics will certainly have an influence

on the nonlinear properties of such materials, but at present there is little evidence to say how significant this is likely to be. Detailed fundamental investigations, for example involving experimental studies of the change in residual stress under an applied electric field, will be necessary in order to clarify this issue.

Acknowledgements

This review was carried out as part of NPL project CPM8.1, *Characterisation of Advanced Functional Materials*. The assistance of Dr M G Cain, Dr M Stewart (NPL) and Dr N Clarke (Materials Science Center) is gratefully acknowledged.

References

1. A. VON HIPPEL, *Rev. Mod. Phys.* **22** (1950) 221.
2. B. LEWIS, *Proc. Phys. Soc. (London)* **73** (1960) 17.
3. R. HERBIET, U. ROBELS, H. DEDERICHS and G. ARLT, *Ferroelectrics* **98** (1989) 107.
4. Y. M. POPLAVKO, V. G. TSYKALOV and V. I. MOLCHANOV, *Sov. Phys. –Solid State* **10** (1969) 2708.
5. A. V. TURIK and N. B. SHEVCHENKO, *Phys. Stat. Sol.* **95** (1979) 585.
6. O. KERSTEN, M. HOFMANN and G. SCHMIDT, *Ferroelectrics Letters* **6** (1986) 75.
7. U. BOTTGER and G. ARLT, *Ferroelectrics* **127** (1992) 95.
8. G. ARLT, U. BOTTGER and S. WITTE, *Ann. Physik* **3** (1994) 578.
9. J. G. SMITS, *IEEE Trans. SU* **23** (1976) 393.
10. Q. M. ZHANG, H. WANG, N. KIM and L. E. CROSS, *J. Appl. Phys.* **75** (1994) 454.
11. D. BERLINCOURT, *J. Acoust. Soc. Am.* **91** 3034.
12. K. CARL and K. H. HARDTL, *Ferroelectrics* **17** (1978) 473.
13. R. HERBIET, H. TENBROCK and G. ARLT, *Ferroelectrics* **76** (1987) 319.
14. G. ARLT, H. DEDERICHS and R. HERBIET, *Ferroelectrics* **74** (1987) 37.
15. S. LI, W. CAO and L. E. CROSS, *J. Appl. Phys.* **69** (1991) 7219.
16. H.-J. HAGEMANN, *J. Phys. C: Solid State Phys.* **11** (1978) 3333.
17. D. A. HALL, *Ferroelectrics* **223** (1999) 319.
18. U. ROBELS, C. ZADON and G. ARLT, *Ferroelectrics* **133** (1992) 163.
19. D. A. HALL and M. M. BEN-OMRAN, *J. Phys.: Condensed Matter* **10** (1998) 9129.
20. LORD RAYLEIGH, *Phil. Mag.* **23** (1887) 225.
21. D. A. HALL and P. J. STEVENSON, *Ferroelectrics* **228** (1999) 139.
22. D. A. HALL, in Minutes of the NPL CAM7 IAG Meeting, NPL, 18th March 1998.
23. D. A. HALL, M. M. BEN-OMRAN and P. J. STEVENSON, *J. Phys.: Condensed Matter* **10** (1998) 461.
24. M. DEMARTIN and D. DAMJANOVIC, *Appl. Phys. Lett.* **68** (1996) 3046.
25. D. DAMJANOVIC and M. DEMARTIN, *J. Phys. D: Appl. Phys.* **29** (1996) 2057.
26. *Idem.*, *J. Phys.: Condensed Matter* **9** (1997) 4943.
27. D. DAMJANOVIC, *Phys. Rev. B* **55** (1997) R649.
28. S. SHERRITT, R. B. STIMPSON, H. D. WIEDERICK and B. K. MUKHERJEE, in Proc. SPIE Far East and Pacific Rim Symposium on Smart Materials, Structures and MEMS, 1996.
29. V. MUELLER and H. BEIGE, *Proc. ISAF'98* (1998) 459.
30. V. MUELLER and Q. M. ZHANG, *Appl. Phys. Lett.* **72** (1998) 2692.
31. V. D. KUGEL and L. E. CROSS, *J. Appl. Phys.* **84** (1998) 2815.
32. S. SHERRIT, H. D. WIEDERICK, B. K. MUKHERJEE and M. SAYER, in SPIE Conference on Smart Structures and Materials 1997 (1997) SPIE Proc. Vol 3040, p. 99.

33. H. H. A. KRUEGER, *J. Acoust. Soc. Am.* **42** (1967) 636.
34. *Idem.*, *ibid.* **43** (1967) 583.
35. H. CAO and A. G. EVANS, *J. Am. Ceram. Soc.* **76** (1993) 890.
36. A. B. SCHÄUFELE and K. H. HÄRDTL, *ibid.* **79** (1996) 2637.
37. C. HEILIG and K. H. HÄRDTL, *Proc. ISAF'98* (1998) 503.
38. N. AURELLE, D. GUYOMAR, C. RICHARD, P. GONNARD and L. EYRAUD, *Ultrasonics* **34** (1996) 187.
39. P. GONNARD, V. PERRIN, R. BRIOT, D. GUYOMAR and A. ALBAREDA, *Proc. ISAF'98* (1998) 353.
40. K. ISHII, N. AKIMOTO, S. TASHIRO and H. IGARASHI, *J. Ceram. Soc. Japan* **106** (1998) 555.
41. W. R. BUESSEM, L. E. CROSS and A. K. GOSWAMI, *J. Am. Ceram. Soc.* **49** (1966) 33.
42. *Idem.*, *ibid.* **49** (1966) 36.
43. M. E. LINES and A. M. GLASS, "Principles and Applications of Ferroelectrics and Related Materials" (Oxford University Press, 1977).
44. J. L. BUTLER and K. D. ROLT, *J. Acoust. Soc. Am.* **96** (1994) 1914.
45. J. ZHAO and Q. M. ZHANG and V. MUELLER, *Proc. ISAF'96* (1996) 971.
46. D. A. HALL, P. J. STEVENSON and S. W. MAHON, *NATO Science Series 3. High Technology* **76** (2000) 149.
47. O. STEINER, A. K. TAGANTSEV, E. L. COLLA and N. SETTER, *J. Eur. Ceram. Soc.* **19** (1999) 1243.
48. P. J. STEVENSON, D. A. HALL and S. W. MAHON, unpublished work.
49. V. PERRIN, M. TROCCAZ and P. GONNARD, *J. Electroceramics* **4** (1999) 189.
50. D. DAMJANOVIC, *Rep. Prog. Phys.* **61** (1998) 1267.
51. S. P. JOSHI, *Smart Mater. Struct.* **1** (1992) 80.
52. D. DAMJANOVIC, *J. Appl. Phys.* **82** (1997) 1788.
53. P. WEISS and D. DE FREUDENREICH, *Arch. Sc. Phys. Nat. Geneve* **42** (1916) 449.
54. F. PREISACH, *Zeitschrift für Physik* **94** (1935) 277.
55. L. NEEL, *Cahiers de Physique* **12** (1942) 1.
56. *Idem.*, *Adv. Phys.* **4** (1955) 191.
57. G. BERTOTTI, "Hysteresis in Magnetism" (Academic Press, 1998).
58. D. JILES, "Introduction to Magnetism and Magnetic Materials" (Chapman and Hall, 1991).
59. H. KRONMULLER, *Z. Angew. Physik* **30** (1970) 9.
60. J. DEGAUQUE, B. ASTIE, J. L. PORTESEIL and R. VERGNE, *J. Magnetism and Magnetic Mater.* **26** (1982) 261.
61. B. ASTIE, J. DEGAUQUE, J. L. PORTESEIL and R. VERGNE, *ibid.* **28** (1982) 149.
62. D. DAMJANOVIC, *NATO Science Series 3. High Technology* **76** (2000) 123.
63. O. BOSER, *J. Appl. Phys.* **62** (1987) 1344.
64. D. DAMJANOVIC, G. ROBERT, J. MULLER, M. DEMARTIN MAEDER, D. V. TAYLOR and N. SETTER, in *Proc. ISAF 2000* (in press).
65. S. C. HWANG, C. S. LYNCH and R. M. McMEEKING, *Acta Metall. Mater.* **43** (1995) 2073.
66. S. C. HWANG, J. E. HUBER, R. M. McMEEKING and N. A. FLECK, *J. Appl. Phys.* **84** (1998) 1530.
67. S. C. HWANG and R. M. McMEEKING, *Int. J. Solids and Structures* **36** (1999) 1541.
68. W. CAO and L. E. CROSS, *Phys. Rev. B* **44** (1991) 5.
69. G. ARLT, *Ferroelectrics* **76** (1987) 451.
70. *Idem.*, *J. Mat. Sci.* **25** (1990) 2655.
71. N. A. PERTSEV and G. ARLT, *Ferroelectrics* **123** (1991) 27.
72. G. ARLT and N. A. PERTSEV, *J. Appl. Phys.* **70** (1991) 2283.
73. G. ARLT, *Ferroelectrics* **189** (1996) 91.
74. *Idem.*, *ibid.* **189** (1996) 103.
75. *Idem.*, *Integrated Ferroelectrics* **16** (1997) 229.
76. T. STEINKOPFF, *J. Eur. Ceram. Soc.* **19** (1999) 1247.
77. C. SCHUH, K. LUBITZ, T. STEINKOPFF and A. WOLFF, *NATO Science Series 3. High Technology* **76** (2000) 391.
78. D. RICINSCHI, C. HARNAGEO, C. PAPUSO, L. MITOSERIU, V. TURA and M. OKUYAMA, *J. Phys.: Condensed Matter* **10** (1998) 477.
79. R. W. JANSE VAN RENSBURG and V. C. HUMBERSTONE, NPL Project AM4: Test Method Development for the High Stress Characterisation of Piezoelectric, Electrostrictive and Magnetostrictive Materials (1996).
80. C. NEWCOMB and I. FLYNN, *Electron. Lett.* **18** (1982) 442.
81. P. GE and M. JOUANEH, *Prec. Eng.* **17** (1995) 211.
82. *Idem.*, *ibid.* **20** (1997) 99.

Received 8 January
and accepted 5 February 2001